Heat Flow in the Western United States

J. H. SASS, ARTHUR H. LACHENBRUCH, ROBERT J. MUNROE,

GORDON W. GREENE, AND THOMAS H. MOSES, JR.

U.S. Geological Survey, Menlo Park, California 94025

Between 1962 and late 1970, subsurface temperature measurements were attempted at more than a thousand drilling sites in the western United States. Temperatures from over 150 boreholes at about 100 distinct sites were suitable for estimates of the vertical geothermal flux. These results more than double the data from the western United States and confirm that heat flow is variable but generally high in this region. Within the over-all pattern of high heat flow, there are several distinct geographical regions, each occupying several hundred square kilometers, characterized by low-to-normal heat flow. Normal values were measured in the Pacific northwestern coastal region and the northwestern Columbia Plateaus. Additional results confirm the previously reported trend of very low heat flow in the western Sierra Nevada, increasing to normal near the crest of the range. The present work also confirms that heat flow is high in the northern and southern Rocky Mountains and somewhat lower in the central Rockies. The north-central part of the Colorado Plateau is a region of normal heat flow with higher values near its eastern border with the southern Rockies. The Basin and Range province as a whole is characterized by high heat flow that extends to within 10 to 20 km of the eastern scarp of the Sierra Nevada. The abrupt thermal transition between the Sierra Nevada and the Basin and Range province may occur partly in the Sierra Nevada physiographic province. Between Las Vegas and Eureka, Nevada, there is a large previously undetected zone of low-to-normal heat flow that is most probably the result of a systematic, regional water circulation to depths of a few kilometers. North of this zone, there is an area of several hundred square kilometers characterized by heat flows of 2.5 HFU (μcal/cm^2 sec) or greater. In central California and adjoining western Nevada, a preliminary contour map suggests a heat-flow pattern with alignment parallel to the strike of the major geologic structures.

Since radioactivity was first discovered, the heat flowing from the earth's deep interior has been considered an important constraint on geophysical and geochemical models of the earth. Until fairly recently, however, the measurement of heat flow on land was accorded a low priority compared with other geophysical measurements, so much so that *Birch* [1954] could report only three reliable measurements for the whole of the United States, and only a dozen or so independent regional determinations (attributable largely to E. C. Bullard and his colleagues) for all the continents. During the late 1950's and 1960's, the early efforts of Francis Birch in the United States, J. C. Jaeger in Australia, and A. D. Misener in Canada, among others, were followed up by these workers, their colleagues, and their students, with the result that the number of reports of reliable heat-flow data from continents is approaching one thousand.

Roy et al. [1968b] recently summarized the work of almost a decade by Birch and his students in the conterminous United States. Their paper included data from almost all major physiographic units, and they were able to make a number of generalizations that heretofore were impossible owing to the scarcity of data. Their results confirmed the earlier observation by L. E. Howard [see *Jaeger and Thyer*, 1960; also, *Howard and Sass*, 1964; *Kraskovski*, 1961] that the heat flow in old shield areas was lower, on the average, than that from younger areas. They also were able to confirm that high heat flow was characteristic of the Basin and Range physiographic province and that low-to-normal heat flow was characteristic of the Sierra Nevada, a result indicated also by independent observations [*Clark*, 1957; *Lachenbruch et al.*, 1966].

The data presented by *Roy et al.* [1968b] have been elaborated and interpreted in papers by *Birch et al.* [1968], *Roy et al.* [1968a],

Decker [1969], *Blackwell* [1969], and *Lachenbruch* [1970]. The discovery that heat flow is a linear function of surface radioactivity for plutonic rocks of the Appalachian region by *Birch et al.* [1968], its independent confirmation for the Sierra Nevada [*Lachenbruch, 1968a*], and its extension to other heat-flow provinces in the United States [*Roy et al., 1968a*] has led to new insights profoundly influencing the interpretation of pre-existing data and the direction of studies initiated since 1968. The results remove much of the ambiguity from estimates of crustal temperatures, mantle heat flow, and vertical distribution of crustal radioactivity. In fact, with a few plausible geologic assumptions, crustal radioactivity beneath plutons is uniquely determined (as exponential), and the other quantities are severely constrained [*Lachenbruch, 1970*]. As a result of these findings, much recent work has focused on plutons and on attempts to establish the limits of validity of the heat flow–heat production relation, but many of the results have not yet reached the published literature.

Decker [1969] amplified the results of *Roy et al.* [1968b] from the central and southern Rocky Mountain area and interpreted them in the light of the geologic history of the region and of the radioactivity (both measured and inferred) of the area. *Blackwell* [1969] made a similar interpretation of his results from the northwestern States and defined the 'Cordilleran Thermal Anomaly Zone' (CTAZ), comprising the northern Basin and Range, the northern Rocky Mountains, and (by interpolation) the Snake River plain. *Warren et al.* [1969], *Spicer* [1964], and *Costain and Wright* [1968] added several data in the Basin and Range and Colorado Plateaus. *Henyey* [1968] presented several values near strike-slip faults in central and southern California. *Combs* [1970] and *Herrin and Clark* [1956] measured heat flow in the western Great Plains.

The work described here grew out of geothermal studies of permafrost terrane begun around 1950. The portion of that study pertaining to heat flow in the Arctic and the related work in other countries has recently been reviewed [*Lachenbruch and Marshall, 1969*]. Heat-flow studies in Alaska are continuing, and they will be reported separately. In this paper we summarize results of measurements begun in the conterminous United States in about 1962. A progress report on these studies involving some 50 determinations at 23 sites in the western United States was given by *Sass et al.* [1968b], and detailed accounts have already been presented for heat-flow results from Menlo Park, California [*Sass et al., 1968c*] and the Sierra Nevada [*Lachenbruch, 1968a*].

Of necessity, *Roy et al.* [1968b] broke with the geothermal tradition of detailed documentation of individual heat-flow data. They presented their data essentially as a summary table in which, for each borehole (or mine or tunnel), the principal elements of the heat-flow calculation and, of course, the heat-flow value itself, were presented in a single line.

The present paper is similar in scope and format to the work of *Roy et al.* [1968b]. It should be noted, however, that a detailed compilation of basic data (temperatures, thermal conductivities, terrain information, etc.) for these and other recent heat-flow determinations from the United States is in preparation, and when published it will allow critical evaluation of recent results from all United States heat-flow groups.

The following symbols and units are used in this paper:

T, temperature, °C.

Γ, vertical temperature gradient $(\partial T/\partial z)$, °C/km.

N, number of thermal conductivity samples.

K, thermal conductivity, mcal/cm sec °C.

R, electrical resistance, ohms.

q, heat flow; 1 heat-flow unit (HFU) = 1 μcal/cm² sec.

$\pm$, refers to the standard error in all cases.

TEMPERATURE MEASUREMENTS

Temperature gradients generally were determined from temperature measurements made at discrete depths in boreholes. The measuring system consisted of a multiconductor cable and hoist, a thermistor thermometer, and a resistance measuring system. In general, measurements were obtained by one of the following three modes of operation:

1. *The well-logging mode.* A truck- or trailer-mounted, hydraulically powered winch with up to 5 km of standard 4-conductor well-logging cable is driven to the site. The truck

contains an instrument rack with the appropriate measuring equipment.

2. *The portable mode.* Some sites are inaccessible by truck or are a long drive from home. In these cases, a portable winch containing up to 1.5 km of light 3-conductor cable armored in stainless steel, which could be backpacked or carried in a light aircraft, is combined with a lightweight (~4 kg) resistance bridge.

3. *The suitcase mode.* This is a compromise between modes 1 and 2, ideally suited to very deep holes at distant locations where commercial well-logging units or other suitable hoist-cable units are available. In this mode, the lightweight resistance bridge, temperature transducers, and suitable adaptors are packed into a suitcase and sent as part of the operator's baggage on common carriers. This mode has been used by one of us (THM) to obtain useful temperature measurements at sites as far apart as Amchitka Island, Mindanao, and Tehran, Iran

[*Sass and Munroe*, 1970; *Sass et al.*, 1971]. The choice among the three modes was usually dictated by logistical requirements, and there is essentially no difference among them in the basic equipment, principles of measurement, or the accuracy of the data obtained. The minor differences that do exist are discussed below.

Figure 1 illustrates the basic principles of the transducers and surface equipment.

Resistance measurement. The resistance bridges (Figure 1a) are all identical in principle to the Siemens variant of the wheatstone bridge illustrated in Figure 1a of *Roy et al.* [1968b]. The bridge compensates almost completely for the series resistance of the cable conductors (there is a small relative error, less than 0.01°C, approximately equivalent to the variation in $|R_1-R_3|$). There is no provision to compensate for the shunt resistance of the cable [see, e.g., *Beck*, 1965] because (1) when the cables were functioning properly, the shunt resistance be-
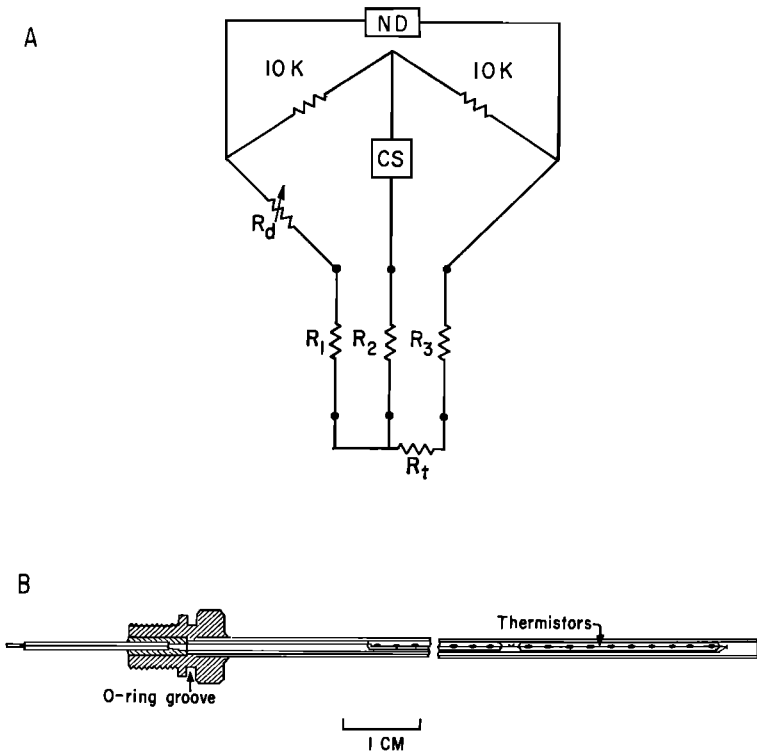
Fig. 1. (a) R_t, thermistor; R_1, R_2, and R_3, lead resistances; R_4, 6-decade variable resistor; CS, current source (1.35-volt mercury cell with voltage divider); ND, battery-operated null detector. (Redrawn from *Roy et al.* [1968b].) (b) Sketch of thermistor probe.

tween individual conductors always exceeded 10 megohms, a value high enough to preclude absolute errors of more than a few hundredths of a degree for the usual range of thermistor resistances (1 to 20 kilohms) and (2) when the shunt resistance fell below a few megohms (usually because of failure of the cable-head), there was a noticeable increase in the noise level of the null detector and difficulty in obtaining a null balance. When this occurred, repairs were effected or another cable unit was substituted for the defective one.

The resistive components of the bridges were chosen for their simplicity of operation, stability, and temperature insensitivity. The various bridges have been compared with one another and with precise secondary standard resistors traceable to the National Bureau of Standards. In no case has the discrepancy in resistance exceeded a few tenths of an ohm. Furthermore, the portable bridges have been operated in conditions ranging from the jungles of Panama and Liberia to the arctic environments of Greenland and the north slope of Alaska without serious operational problems.

Temperature transducers. Figure 1b illustrates the essential features of the thermistor probe assembly that formed the basis of most temperature sondes. It is basically a stainless steel tube 0.4 cm in outer diameter and 15 cm long containing, in its lower 9 cm, a series-parallel network of 20 thermistor beads having a nominal resistance of 8 to 10 kΩ at 20°C and a temperature coefficient of resistance of about $-4\%/°C$. The thermistor section is filled with a silicone lubricant of low viscosity, which facilitates thermal contact with the probe wall. An air space is left above the thermistor section to accommodate the compressive stresses encountered in deep holes without transmitting them to the thermistors. The probe has a time constant of about 2 sec in still water and will dissipate 100 μw in still water with a temperature rise of less than 10^{-3}°C. Recent advances in solid-state technology have resulted in rugged, portable, and inexpensive electronic null detectors capable of a sensitivity of 10^{-4}°C with a current of only a few μa, so that the high-power dissipation characteristic is no longer important, and single beads can be used.

For modes 1 and 3, the sondes were constructed by machining a 9-cm length of cylindrical stock (SAE #4130 steel or Lexan, a high-impact–strength plastic), 2.54 cm in diameter to accommodate one- or three-probe assemblies at one end and a cablehead of 2.54-cm diameter at the other. In the three-element variety the sonde could be operated with only one element in the circuit or with all three elements in series (this to preserve sensitivity at high temperatures). The mode 2 sondes were simply aluminum cableheads that were 8 cm long and 1.27 cm in diameter, fitted to a single thermistor assembly with O-ring seals.

For all modes, slotted metal 'sinker bars' were attached to the cable above the sonde to provide line tension and/or to aid in penetration of viscous well fluids. With metal cableheads, a short (20- to 30-cm) length of 'Lexan' was usually inserted between the sonde and the sinker-bar column to thermally decouple the sonde from the sinker bars. In modes 1 and 3, the winches were fitted with high-quality slip rings that allowed continuous monitoring of the transducers. In mode 2, considerations of weight versus contact resistance resulted in the sacrifice of this convenience, and a signal lead was plugged in to the winch when the cable was stationary. Temperatures were measured at regular discrete intervals ranging from less than 1 meter (for short-cored intervals) to 15 meters in deep holes (>1 km) in crystalline rocks.

Thermistor calibration. Most thermistor probes were calibrated at the factory at 10° intervals between $-10°$ and $+150°$C. The precision of each calibration point was about ±0.1°C, but by fitting a series of segments of the form

$$T = (A/\text{Log } R + B) - C \qquad (1)$$

to overlapping 30° temperature ranges and adjusting erroneous values to produce smooth fits, it was possible to obtain values of A, B, and C for which differential temperatures for the same thermistor could be calculated to a precision of better than 0.01°C. This precision is adequate for most heat-flow purposes. There are, however, some instances where very high precision is required. These include precise temperature-gradient determinations at $\sim$1-meter intervals, measurements near the freezing point in permafrost terranes, and measurements at different levels in mines using different sondes. To be prepared for these cases, most thermistors

were recalibrated over the range $-10°$ to $80°$ or $100°C$ in our laboratory. The recalibrations were made at $10°$ intervals, but to a precision of ± 1 or $2 \times 10^{-3}°C$ relative to a standardized platinum resistance thermometer. This thermometer was checked, in turn, in a triple-point cell every three to four months. For the past three years, the platinum standard has been drifting upward fairly steadily at the rate of about $0.01°C$/year, and the appropriate corrections have been applied to thermistors. Recent batches of thermistor probes have proved extremely stable, with drift rates of $0.01°C$/year or less when operated in the temperature range of $-10°$ to $+150°C$.

The recalibrated thermistors give values of A, B, and C (equation 1) for which the precision of differential temperatures approaches the sensitivity of the system ($10^{-4}°C$). The error in absolute temperature is more difficult to assess because of the many possible sources of error; however, on the basis of repeated measurements in the same hole with different probes and cables, and of comparisons with independent measurements by systems claiming a similar relative accuracy (R. F. Roy, personal communication), the error in absolute temperature is probably only a few hundredths of a degree, and certainly is no greater than one or two tenths of a degree centigrade in the worst case.

Some of the early temperature measurements were made with strings of thermistors originally designed to be frozen in place in Arctic locations [see Lachenbruch et al., 1962]. With these, the temperatures at successive depths were measured with different thermistors, and errors of up to $0.1°C$ could occur in the temperature difference between adjacent thermistors, although they were usually much smaller. The high relative error does not seriously affect temperature-gradient estimates when these are determined by least-squares straight-line fits, as was done in most of this work.

THERMAL CONDUCTIVITY

By far the majority of thermal-conductivity measurements were made with the modified Birch-type [Birch, 1950] divided-bar apparatus described below.

With soft and poorly consolidated rocks, the needle-probe technique [Von Herzen and Max-

well, 1959] was used to determine conductivity. The probe system is used routinely for conductivity determinations on ocean-bottom cores and was described by Lachenbruch and Marshall [1966]. Whenever possible, the samples were sealed in plastic tubes (which, in turn, were dipped in paraffin wax) immediately after being removed from the ground to preserve their moisture content.

The quality of the needle-probe data varied considerably. Fine-grained, clayey sediments gave satisfactory results, but for pebbly sediments, there were contact problems and problems associated with the size of particles relative to the volume sampled by the probe. In some instances, the sample had been allowed to dry, and water was introduced prior to measurement. In the most favorable cases, needle-probe determinations were very precise ($\pm 1\%$). A more common uncertainty is probably about $\pm 10\%$, with errors of $\pm 20\%$ possible in some 'problem' cases.

For many holes, the only samples available were drill cuttings. For others, the rock was so badly weathered or so poorly cemented that suitable disks could not be prepared for the divided bar, but the grains were too hard to permit drilling of the long small-diameter holes required for a needle-probe determination. In these instances, conductivities were measured on fragments using the chip technique described by Sass et al. [1971]. For a given determination, this technique has an over-all accuracy of $\pm 10\%$, which is adequate in view of the fact that the standard deviation of a single (precise) conductivity determination due to compositional heterogeneity on the scale of a few centimeters is of the same order.

The divided-bar apparatus. The apparatus consists of four units of the type depicted schematically in Figure 2, connected in parallel to a pair of constant-temperature baths. The cylindrical elements usually are either 3.81 cm or 2.86 cm in diameter. The basic principles of operation of this apparatus are well known [see, e.g., Birch, 1950]. Briefly, cylindrical rock specimens of unknown conductivity are placed in series with copper disks containing wells for temperature transducers and with standard disks of known conductivity (0.3-cm-thick fused silica disks in this case). The extreme ends of this 'stack' are held at different, constant tem-

peratures, the entire apparatus is allowed to achieve a thermal steady state, and the temperature drops across standard disks are compared with those across samples of unknown conductivity. The latter conductivity is determined from the ratios of the temperature drops and thicknesses between sample and standard. In the configuration illustrated in Figure 2, the conductivities of two unknowns are determined simultaneously.

The apparatus was calibrated using *Ratcliffe's* [1959] values for quartz and fused silica as standard values. It was usually operated at a mean temperature of about 25°C, with a total temperature drop of 7° to 10°C between the warm and the cold baths. Over a period of 20 minutes or so (the average duration of a determination), each bath can be maintained at a mean temperature constant to within a few thousandths of a degree. Short-period (∼1 to 10 sec) variations of up to a few hundredths of a degree are damped out by 0.2-cm-thick disks of Micarta (laminated plastic and linen) at each end of the stack.

The divided bar is very simple in principle, but there are two practical problems that must be carefully managed to avoid large errors. These are radial heat losses and contact resistance. The first is minimized by careful lagging with styrofoam. Three procedures are followed to reduce contact resistances to negligible levels.

1. The faces of all disks are made as flat and as parallel as possible. For standards and copper disks the tolerances are ±0.0005 cm. For samples they are relaxed to ±0.002 cm for flatness and ±0.005 cm for parallelism. (The rubber pad beneath the cold bath, shown in Fig. 2, easily accommodates wedges of this magnitude.)

2. The faces of all disks are coated with a very thin film of a paste or liquid of relatively high conductivity (1 or 2 mcal/cm sec °C). A commercial mixture of silicone grease and metal oxide or a liquid household detergent were used as contact films.

3. Axial pressure of 80 to 100 bars is applied to the stack to extrude the excess contact material and to minimize the variation in contact resistance within a series of determinations.
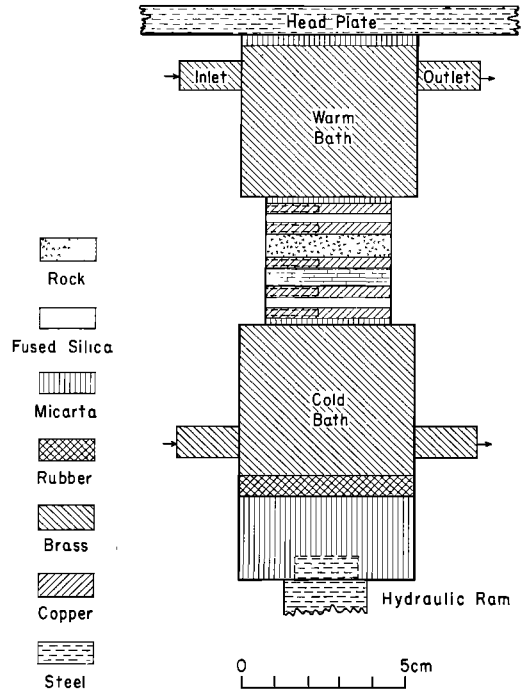
Fig. 2. Schematic representation of the divided-bar apparatus. The dashed lines in the copper sections are projections of cylindrical thermistor wells.

Walsh and Decker [1966] have demonstrated that even for rocks of low porosity, significant errors in conductivity can result if the rocks are not saturated (their normal condition in situ). All rocks were saturated with water under vacuum prior to measurement.

For many rocks, thermal conductivity is sufficiently sensitive to temperature that corrections must be made if the in situ temperature is more than 5° or 10°C different from that at which the conductivity determination is made. The temperature coefficients of thermal resistivity for a number of common rocks were determined by *Birch and Clark* [1940]. Checks between 20° and 50°C on a few of the samples from the present work gave values consistent with those of Birch and Clark, and the appropriate coefficients were used in correcting the measured conductivity to in situ temperatures.

CALCULATION OF HEAT FLOW

In general the heat flow q is obtained by combining in some way the measured thermal

conductivities and temperature gradients according to

$$q = K\Gamma \qquad (2)$$

The most appropriate way of doing this depends on the actual distribution of conductivity and temperature with depth and on how well these distributions are known at any site. The common methods of data reduction are reviewed by *Hyndman and Sass* [1966]. The three methods that were used in this study are described in detail in the next section.

The quantity determined from (2) is usually referred to as the uncorrected heat flow. It is based on the assumption that all the heat transfer is by one-dimensional steady-state conduction. Departures from this condition can lead to local heat-flow determinations quite unrepresentative of the regional vertical conductive flux. An effort was made to identify such departures at each site and either to account for them or to allow for them in evaluating the reliability of the determinations. Effects considered include vertical water flow [see e.g., *Birch*, 1947; *Bredehoeft and Papadopulos*, 1965], drilling disturbance [*Bullard*, 1947; *Lachenbruch and Brewer*, 1959; *Jaeger*, 1961], climatic change [*Birch*, 1948], uplift, erosion, and sedimentation [*Birch*, 1950; *Jaeger*, 1965], effects of lakes, rivers, and other regions of anomalous surface temperature [*Lachenbruch*, 1957a, b], and the steady-state effects of topographic relief and thermal refraction in dissimilar rocks. Only the last two warrant discussion here. It is important, however, that many conditions leading to nonconductive, transient, or two- and three-dimensional heat flow can go undetected, and this must certainly contribute to the scatter of internally consistent heat-flow determinations.

Topographic corrections. Topographic relief can distort the temperature field sufficiently to cause errors in heat-flow determinations. The map reading involved in detailed topographic corrections is very tedious, and it is often impossible to judge, simply by looking at a topographic map, whether the effects are significant. In view of this, we considered the problem of terrain correction in two stages. If topographic relief in the area exceeded a few tens of meters, we made a preliminary estimate of its steady-state effect based on an exaggerated two-dimensional approximation to the true topography. The approximations were Lees-type hills, valleys, or monoclines [see *Jaeger and Sass*, 1963] or plane slopes [*Lachenbruch*, 1968b]. In the rare instances where the two-dimensional representation seemed a reasonable approximation to the true topography (some ridges and fault scarps, or fairly distant relief) this correction was used. In the majority of cases, however, the two-dimensional correction was not used. If it did not exceed 5% (about 70% of the cases), no topographic correction was made. If it did exceed 5%, a three-dimensional Birch-type correction [*Birch*, 1950] was performed in which the effect of all topography outward from the borehole collar to at least 90% of the solid angle subtended by the lowest temperature measurement point was calculated. These corrections were invariably substantially smaller than the two-dimensional approximations, so that we felt justified in ignoring topography where the latter correction was 5% or less. It should be noted that the first-order correction of *Birch* [1950] can result in large errors if steep slopes occur at or near the station [see e.g. *Lachenbruch*, 1968b].

For all topographic corrections, we assumed that the ground-surface temperature decreased 5°C/km with increasing elevation, a generalized value obtained from weather bureau records and from shallow holes. Although this simple one-dimensional model can introduce significant errors in rare cases [see, e.g., *Blackwell*, 1969], the available information on local variations is usually too scant to define the exact local conditions, and the simple assumption is the best that can be made.

Refraction. When heat flow is determined from measurements near steeply inclined contacts between rocks of contrasting conductivity, the one-dimensional interpretation can result in substantial errors. Heat flow will be underestimated if the measurements are in the lower conductivity rocks and overestimated for measurements in the higher conductivity rocks. *Howard and Sass* [1964] discussed an example of a probable underestimate of nearly 100% near Rum Jungle in northern Australia.

Corrections for refraction are sensitive to geometric details that are usually unknown; however, rough estimates of its effect can often

be obtained from simple models [see e.g., *Roy*, 1963; *Hyndman and Sass*, 1966; *Sass et al.*, 1968a; *Von Herzen and Uyeda*, 1963; *Lachenbruch and Marshall*, 1966]. In a region like the Basin and Range province, where alluvial valleys conceal down-faulted bedrock pediments that can have conductivities three or four times as high as the valley sediments, refraction anomalies can be very large [see *Lachenbruch*, 1968b, p. 399]. A series of measurements near Tucson, Arizona (discussed below), provides an example of the probable effects of unknown conductivity structure.

THE HEAT-FLOW VALUES

The heat-flow values are presented in Tables 1 through 8, one table for each major physiographic-tectonic province in the western United States. The boundaries of these provinces, based on those of *Fenneman* [1928] are shown in Figure 3, together with the locations of previously published heat flows and the present values. (See also Figure 4.)

In most papers on heat flow, the standard error or some other statistical measure of scatter is calculated for each of the principal elements of the heat-flow calculation (conductivity and temperature gradient). These are combined in some way to arrive at a formal statistical estimate of the reliability of the heat-flow value. It is then pointed out that the formal standard error does not adequately take account of the possible sources of error, but that (hopefully) the values are accurate to within some reasonable limits. This is the general procedure followed here, but we have defined three broad categories to take some account of the large range of quality among the data. In assigning a heat flow to one category or another we were guided by the objective general criteria listed below, but, in some borderline cases, rather subjective judgments based on experience in other areas decided the issue.

Each of the eight tables presents data in at least one of the following three categories:

Category 1. These are determinations of the highest quality. Temperature profiles are smooth, with no sign of hydrologic disturbances below depths of a few tens of meters. Sufficient samples of rock are available to characterize the effective conductivity of the measured

section, and no variations that cannot be explained and corrected are apparent. If conductivity stratification is present, component heat flows for the various individual strata are in good agreement. Typical uncertainties for category 1 are less than ±10%.

Category 2. For this category, the uncertainty in heat flow is greater than for category 1, but it probably is no greater than ±20%. Included here are temperature profiles in which there are suggestions of local hydrologic disturbances. Also included are cases where the conductivity sample is unsatisfactory, owing to either too few samples or an unusually large scatter in conductivity values. In the stratified cases, if component heat flows do not agree satisfactorily and there is not enough structural information to resolve the disagreement with refraction calculations, the average of the components is taken and the value is relegated to this category.

Category 3. Values in this category are little more than rough estimates, and, taken individually, they do not yield much information. When combined with higher-quality data on a regional basis, however, these heat flows can be quite useful. In the tables, the values in category 3 are given to the nearest 0.5 HFU. The implication here is that the uncertainty is of this order. For some of the higher values, the uncertainty can exceed 1 HFU. Category 3 values are shown within parentheses in the relevant figures to emphasize the point that they are merely estimates.

For each site, the principal elements of the heat-flow calculation are given in Tables 1 through 8. Each table consists of twelve columns. The first four columns identify the location of the site by name, hole, or well number (where appropriate), latitude and longitude to the nearest minute, and surface elevation. Column 5 gives the depth range applicable for each line of the table. The columns headed N and K refer to the number of conductivity specimens and the arithmetic mean conductivity (± standard error), respectively. If most conductivities in a given set were obtained by measurements on solid disks with the divided-bar apparatus, the average conductivity is not flagged in any way. The superscripts f and n in the K column denote that the majority of

TABLE 1. Heat Flow from the California Coastal Province

Locality	North Latitude	West Longitude	Elevation, meters	Depth Range, meters	N	K, mcal/cm sec °C	Γ, °C/km	q(unc), HFU	q(corr), HFU		
									Category 1	Category 2	Category 3
Fort Bragg	39° 26'	123° 44'	120	444–1207	0	~4*	48.3 ±6.5	2			2
Willitts (EC-1)	39° 34'	123° 07'	1100	153–344	6	8.41 ±0.28	21.40 ±0.06	1.80 ±0.06	1.8		
Cold Creek (EG-8)	39° 42'	122° 53'	1186	175–327	10	10.3 ±0.5	20.43 ±0.05	2.11 ±0.10	1.6		
Cottonwood Glade (EG-7)	39° 42'	122° 48'	1585	220–1245	39	6.95 ±0.31	16.2 ±0.02	1.13 ±0.05	1.17		
Berkeley (BER)	37° 52'	122° 15'	122	33–159	6	5.0 ±1.0	36.74 ±0.07	1.84 ±0.4			2
Tracy (TRA)	37° 48'	121° 35'	19	33–246	34	3.27[a] ±0.14	(29.3)[b]	0.96 ±0.02	0.96		
Menlo Park	37° 27'	122° 10'	16	68–218	165	3.99[a] ±0.03	(54.1)[i]	2.16	2.16		
				218–240	53	5.1 ±0.5	42.5 ±0.2	2.2 ±0.2	2.2		
				Best value					2.2		
Dumbarton SF Bay #1	37° 29'	122° 08'	1	114–117	10	3.72[a] ±0.15	63.85 ±0.78	2.37 ±0.10	2.4		
				155–157	5	4.13[a] ±0.13	51.5 ±2.1	2.13 ±0.11	2.1		
				Mean					2.25		
Sunnyvale (SV)	37° 27'	122° 02'	12	160–258	42	3.44[a] ±0.06	58.6 ±0.6	2.02 ±0.04	2.02		
Permanente 586	37° 19'	122° 07'	509	183–204	7	6.40[f] ±0.49	21.87 ±0.65	1.40 ±0.11		1.9	
659			483	92–155	21	10.05[f] ±0.25	12.03 ±0.22	1.21		2.2	
				155–181	11	7.04[f] ±0.38	27.6 ±0.8	1.94 ±0.12		2.4	
				Mean (2 holes)						2.2	
La Panza (TS)	35° 26'	120° 30'	427	76–166	14	6.90 ±0.16	32.90 ±0.66	2.25 ±0.07	2.06		

TABLE 1. (continued)

Locality	North Latitude	West Longitude	Elevation, meters	Depth Range, meters	N	K, mcal/cm sec °C	Γ, °C/km	q(unc), HFU	q(corr), HFU Category 1	Category 2	Category 3
Elk Hills											
366-24Z	35° 18'	119° 34'	365	1782–1864	22	5.08* ±0.16	19.2 ±0.8	0.98 ±0.05	1.0		
385-24Z	35° 18'	119° 33'	361	1496–1756	20	3.76* ±0.28	(31.1)[i]	1.17 ±0.05	1.2		
326-28R	35° 17'	119° 31'	441	685–838	7	3.58[f] ±0.25	36.9 ±1.0	1.32 ±0.10			
				1420–1850	23	3.47* ±0.08	35.81 ±0.20	1.24 ±0.03			
				Mean					1.26		
372-35R	35° 17'	119° 28'	405	2098–2113	6	4.90* ±0.15	(27.3)[i]	1.34 ±0.14		1.3	
343-4G	35° 16'	119° 24'	317	1391–2142	26	3.82* ±0.16	(29.3)[i]	1.12 ±0.03	1.12		
382-3G	35° 16'	119° 23'	277	2115–2141	5	4.23* ±0.35	(32.2)[i]	1.36 ±0.20			
				2207–2231	19	4.58* ±0.16	27.10 ±0.30	1.24 ±0.04	1.26		
344-35S	35° 17'	119° 22'	222	2091–2152	7	4.05* ±0.28	(28.4)[i]	1.15 ±0.25		1.2	
				Mean							
Los Angeles Basin (LB-1)	33° 53'	118° 02'	21	2073–3223	40	5.04 ±0.16	34.5 ±0.1	1.75 ±0.05	1.74		
Santa Ana AC-1	33° 58'	117° 38'	300	30–183	17	3.6* ±0.1	46.0 ±2.2	1.66 ±0.09			
				183–305	13	2.35* ±0.04	64.2 ±2.9	1.51 ±0.07			
				Mean							1.6

Definitions (applicable to Tables 1–8): q(corr), corrected heat flow; q(unc), uncorrected heat flow; superscript b, Bullard method; superscript f, measured on fragments; superscript i, interval method; superscript n, needle-probe method.
  * Estimated conductivity.

TABLE 2a. Heat Flow from the Sierra Nevada

Locality	North Latitude	West Longitude	Elevation, meters	Depth Range, meters	N	K, mcal/cm sec °C	Γ, °C/km	q(unc), HFU	q(corr), HFU Category 1	Category 2	Category 3
Moonlight Valley											
ML-9	40° 13'	120° 48'	1710	238–334	15	7.99 ±0.25	19.64 ±0.19	1.57 ±0.05		1.60*	
ML-43	40° 14'	120° 48'	1670	46–148	14	8.11 ±0.36	24.97 ±0.13	2.03 ±0.09	1.92		
San Juan Ridge				Best value					1.9		
SJR-1	39° 24'	120° 52'	1378	246–256	6	7.84 ±0.14	8.79 ±0.11	0.69 ±0.02	0.65		
SJR-2	39° 24'	120° 53'	1406	274–276	9	13.0 ±1.0	5.74 ±0.05	0.75 ±0.06		0.72	
Auburn Dam				Mean					0.69		
AD-34	38° 52'	121° 03'	295	30–183	20	9.00 ±0.10	15.05 ±0.27	1.35 ±0.03		0.72†	
AD-117	38° 53'	121° 03'	150	44–152	12	8.65 ±0.30	(17.7)‡	1.53 ±0.11		0.72‡	
AD-212	38° 53'	121° 03'	157	60–130	19	7.17 ±0.17	(19.8)‡	1.42 ±0.06		0.67‡	
				Mean						0.70	
Sherman Thomas Ranch (ST)	37° 10'	120° 04'	110	203–488	90	7.13 ±0.04	6.35 ±0.02	0.45 ±0.01	0.45		
San Joaquin Experimental Range (SJ)	37° 06'	119° 44'	335	280–459	201	6.97 ±0.06	8.90 ±0.04	0.62 ±0.01	0.61		
Jose Basin (JB)	37° 06'	119° 23'	1000	201–491	191	6.05 ±0.03	12.2 ±0.03	0.74 ±0.01	0.77		
Helms Creek (HC)	37° 08'	118° 59'	2510	60–490	203	7.09 ±0.03	17.2 ±0.01	1.22 ±0.01	1.30		

* There is evidence for downward water movement above 238 meters.
† Correction made for 1°C temperature drop about 80 years ago. The drop could have been caused by a landslide or by hydraulic mining operations.
‡ On the edge of a river; corrections made assuming a temperature difference of 4°C between land and water.

TABLE 2b. Heat Flow from the Tehachapi Mountains

Locality	North Latitude	West Longitude	Elevation, meters	N	Depth Range, meters	K, mcal/cm sec °C	Γ, °C/km	q(unc), HFU	q(corr), HFU Category 1	Category 2	Category 3
Tejon Ranch, California											
DH-61	34° 57'	118° 49'	506	9	107–153	7.23 ±0.24	18.4 ±2.1	1.33 ±0.16		1.31	
DH-62	34° 56'	118° 49'	476	10	76–130	6.35 ±0.44	23.93 ±0.39	1.52 ±0.11	1.33		
DH-65	34° 56'	118° 49'	791	31	244–433	6.95 ±0.25	18.51 ±0.08	1.29 ±0.05	1.38		
					Mean (3 holes)				1.36		
DH-43	34° 53'	118° 46'	1119	6	122–183	8.13 ±0.26	21.75 ±0.09	1.77 ±0.06	1.83		

TABLE 3. Heat Flow from the Pacific Northwest Coastal Province

Locality	North Latitude	West Longitude	Elevation, meters	N	Depth Range, meters	K, mcal/cm sec °C	Γ, °C/km	q(unc), HFU	q(corr), HFU Category 1	Category 2	Category 3
Chehalis, Washington											
SU-4	46° 32'	122° 50'	165	59*	100–380	2.58* ±0.1	32.8 ±0.2	0.85 ±0.03			
				5	710–760	4.23 ±0.03	19.4 ±0.6	0.82 ±0.02			
SU-11			157	59	100–340	2.56* ±0.1	34.6 ±0.2	0.89 ±0.04			
SU-14			156	59	100–400	2.56* ±0.1	33.8 ±0.1	0.86 ±0.03			
				77	Best value	2.74* ±0.10	(30.3)				0.83

* Core was obtained from SU-4 and from four other wells, all of which were within a few hundred meters of the holes in which temperatures were measured.

TABLE 4. Heat Flow from the Columbia Plateaus

Locality	North Latitude	West Longitude	Elevation, meters	Depth Range, meters	N	K, mcal/cm sec °C	Γ, °C/km	q(unc), HFU	q(corr), HFU Category 1	Category 2	Category 3
Nevada											
White Elephant Butte, EB-1	41° 53'	115° 05'	2010	100–366	7	8.68 ±0.28	43.4 ±0.2	3.76 ±0.12		3.3*	
Washington											
Rattlesnake Hills	46° 26'	119° 47'	875								
RS-1				900–2500	6	3.75 ±0.3	(34.8)ⁱ	1.31 ±0.1		1.39	
RS-2				58–119	14	4.12 ±0.10	28.0 ±0.2	1.15 ±0.03	1.36		
				Best value (2 holes)					1.4		
Richland DH-3	46° 21'	119° 17'	120	305–608	16	3.95 ±0.17	38.95 ±0.15	1.54 ±0.07	1.54		
				608–1079	15	3.64 ±0.08	34.58 ±0.28	1.26 ±0.03		1.3	
Willa, DH-1	46° 35'	119° 31'	168	Best value 53–183	19	4.08 ±0.08	37.2 ±0.3	1.52 ±0.03	1.5 1.52		

* Water flowing steadily from the collar at about 2 to 3 liters/minute [cf. Birch, 1947].

TABLE 5. Heat Flow from the Colorado Plateau Province

Locality	North Latitude	West Longitude	Elevation, meters	Depth Range, meters	N	K, mcal/cm sec °C	Γ, C/km°	q(unc), HFU	q(corr), HFU Category 1	Category 2	Category 3
Colorado Yellow Creek											
CH-1	40° 03'	108° 20'	1830	46–671	25	3.40 ±0.26	43.3 ±0.2	1.47 ±0.11			
				671–881	14	2.25 ±0.25	63.4 ±0.9	1.43 ±0.16	1.5		
				Mean							
CH-2	39° 58'	108° 28'	2011	76–404	10	3.42 ±0.28	30.1 ±0.2	1.03 ±0.08			
				404–488	6	2.58	57.0	1.47			
				663–716	5	2.52 ±0.27	50.9 ±0.3	1.28 ±0.15			
						±0.39	±1.9	±0.20			
				Best value						1.4	
CH-3	40° 03'	108° 21'	1937	617–983	14	2.64 ±0.21	56.4 ±0.7	1.49 ±0.12	1.5		
Barcus Creek BC-1	40° 03'	108° 31'	1920	411–544	17	2.87 ±0.36	67.4 ±0.7	1.93 ±0.24			2*
Rio Blanco TG2-3	39° 46'	108° 09'	2070	46–107	8	3.79 ±0.16	57.9 ±0.4	2.19 ±0.09			
				201–322	16	2.69 ±0.20	49.4 ±1.4	1.33 ±0.11			
				Mean							1.5
New Mexico Gobernador GB-1	36° 41'	107° 12'	2194	1052–1288	9	6.6 ±0.8	(30.6)*	2.02 ±0.08	2.01		
Utah Ouray W-Ex-1	39° 59'	109° 36'	1520	61–533	11	5.63' ±0.17	25.13 ±0.06	1.42 ±0.04			
				541–907	51	4.90 ±0.18	32.19 ±0.28	1.60 ±0.06			
				Mean					1.50		

* Strong vertical water movement above 400 meters.

TABLE 6. Heat Flow from the Rocky Mountain Province

Locality	North Latitude	West Longitude	Elevation, meters	Depth Range, meters	N	K, mcal/cm sec °C	Γ, °C/km	q(unc), HFU	q(corr), HFU Category 1	Category 2	Category 3
Colorado											
Rocky Mountain Arsenal, Denver	39° 51'	104° 51'	1501	368–2535	42	5.83' ±0.65	(38.6)ⁱ	2.25 ±0.11		2.14	
				3017–3597	19	8.96 ±0.60	24.7 ±1.0	2.21 ±0.16		1.88	
			Mean								2.0
Idaho											
Galena mine, Wallace (GAL)	47° 29'	115° 58'	928	957–1201	30	11.9* ±1.8	21.42 ±0.01	2.55 ±0.38		2.3	
Montana											
Verdigris Creek Hole M-22	45° 23'	109° 54'	2151	83–209	24	8.80 ±0.17	17.8 ±0.1	1.57 ±0.03	1.63		
Hole M-19A	45° 23'	109° 55'	2140	111–171	11	8.4 ±0.4	16.9 ±0.2	1.42 ±0.07	1.35		
				171–269	21	7.15 ±0.21	21.2 ±0.2	1.52 ±0.05	1.47		
				Mean (2 holes)					1.52		
Nye Basin Hole NB-2	45° 22'	109° 49'	2470	163–253	6	7.8 ±0.4	18.7 ±0.4	1.46 ±0.08	1.39		
Wyoming											
Pinedale (DHPW)	42° 46'	109° 34'	2218	305–1356	27	7.21 ±0.26	19.21 ±0.04	1.38 ±0.05	1.38		
				2088–2996	29	6.79 ±0.12	16.41 ±0.03	1.14 ±0.02	1.25		
			Mean						1.3		
Green River (GR1-1)	41° 32'	109° 25'	1890	53–152	7	3.64 ±0.34	44.1 ±0.8	1.61 ±0.15	1.6		

* Temperatures were measured near a vertical contact between rocks of contrasting conductivities. The standard error in conductivity includes the uncertainty in the structural effect.

TABLE 7. Heat Flow from the Great Plains Province

Locality	North Latitude	West Longitude	Elevation, meters	Depth Range, meters	N	K, mcal/cm sec °C	Γ, °C/km	q(unc), HFU	q(corr), HFU Category 1	Category 2	Category 3
Kansas											
Lyons					91*	7.93ʰ ±0.42					
Hole 1	38° 23'	98° 10'	525	99–229		3.82 ±0.38	36.42 ±0.56	1.39 ±0.14			
				252–328		12.5 ±1.0	13.35 ±0.20	1.67 ±0.14			
Hole 2	38° 22'	98° 10'	512	128–212		3.70 ±0.37	40.84 ±0.30	1.51 ±0.15			
				235–311		11.9 ±1.0	12.63 ±0.21	1.50 ±0.13			
				Mean (2 holes)					1.50		
South Dakota											
Windy Flats Hole NBH-1	44° 18'	103° 40'	1652	383–516	7	5.12 ±0.29	9.10 ± 0.07	0.47 ±0.03		0.5	
Moonshine Gulch Hole NBH-2	44° 08'	103° 43'	1695	126–250	13	6.70 ±0.46	7.77 ±0.04	0.52 ±0.04		0.5	
Dacy Hole RTM-1	44° 22'	103° 53'	1790	204–334	7	7.3 ±1.0	25.6 ± 0.05	1.87 ±0.26		1.9	

* The holes penetrated interbedded, flat-lying, sedimentary layers of contrasting conductivities. An arithmetic mean conductivity was calculated for each distinct rock type. These averages were used, together with relative abundances from detailed core logs, to calculate a harmonic mean conductivity for each gradient interval.

TABLE 8. Heat Flow from the Basin and Range Province

Locality	North Latitude	West Longitude	Elevation, meters	Depth Range, meters	N	K, mcal/cm sec °C	Γ, °C/km	q(unc), HFU	q(corr), HFU Category 1	Category 2	Category 3
Arizona											
Yuma											
LCRP-26	32° 44′	114° 37′	50	220–338	15	5.6 ±0.5	34.3 ±1.1	1.92 ±0.18		1.92	
LCRP-13	32° 41′	114° 37′	60	30–137	7	5.0 ±0.5	44.9 ±0.5	2.24 ±0.22			
				137–223	3	5.3 ±0.5	35.6 ±1.2	1.88 ±0.19			
				Mean				2.06		2.1	
Phoenix	33° 32′	112° 20′	331	107–229	9	3.7ᶠ ±0.5	85.9 ±0.5	3.18 ±0.43			
ST-1				238–268	6	8.1ᶠ ±0.4	50.9 ±1.1	4.12 ±0.22			
				268–1365	0*	13.0 ±1.0	14.8 ±1.0	1.92 ±0.20			
				Mean				2.06			>3
Tempe A-1-3	33° 25′	112° 01′	340	107–175	4	3.7* ±0.5	29.6 ±0.2	1.09 ±0.15		1.1	
Higley D-1-6	33° 19′	111° 43′	395	100–280	22	3.79ᶠ ±0.11	45.7 ±0.6	1.73 ±0.06		1.7	
Red Rock	32° 36′	111° 36′	500	100–260	2	2.8ᵃ ±0.2	30.19 ±0.25	0.85 ±0.06			
D-9-7				260–353	6	3.77 ±0.30	22.6 ±0.4	0.85 ±0.07			
				Mean					0.85		
Eloy D-7-8	32° 47′	111° 29′	480	200–230	6	3.70ᵃ ±0.33	34.2 ±0.2	1.27 ±0.11	1.3		
Christmas SM-1	33° 02′	110° 41′	762	168–320	12	7.61 ±0.33	18.84 ±0.15	1.43 ±0.11	1.4		
San Manuel DH-34	32° 40′	110° 42′	1053	914–1372	42	8.72 ±0.58	17.61 ±0.14	1.54 ±0.11	1.54		
Tucson KCL-7	32° 11′	111° 07′	795	152–442	70	8.61 ±0.34	29.69 ±0.14	2.56 ±0.06	2.56		
Helmet Peak A-545	31° 58′	111° 04′	1033	91–335	8	8.09 ±0.29	26.40 ±0.08	2.14 ±0.09	2.14		
Twin Buttes A-644	31° 54′	111° 03′	1017	198–472	46	9.31 ±0.23	22.6 ±0.07	2.10 ±0.06	2.10		
A-911	31° 54′	111° 02′	1025	137–366	43	8.37 ±0.29	23.7 ±0.3	1.98 ±0.07	1.98		

TABLE 8. (continued)

Locality	North Latitude	West Longitude	Elevation, meters	Depth Range, meters	N	K, mcal/cm sec °C	Γ, °C/km	q(unc), HFU	q(corr), HFU Category 1	Category 2	Category 3
Arizona (continued)											
A-616	31° 53′	111° 02′	1010	183–396	23	8.82 ±0.42	21.3 ±0.3	1.88 ±0.09	1.88		
A-940	31° 53′	111° 02′	993	183–335	31	7.48 ±0.22	20.9 ±0.2	1.56 ±0.05	1.56		
California											
Black Rock BR	37° 41′	118° 32′	2110	183–206	0	6*	33.5 ±1.6	2.0			2
Deep Springs DS-1A	37° 24′	118° 00′	1630	250–305	55	6.6 ±0.7	28.76 ±0.27	1.89 ±0.20		1.8	
Eagle Mountain CK-3	33° 52′	115° 26′	285	350–426	10	6.48 ±0.22	19.9 ±0.5	1.29 ±0.05	1.29		
Nevada											
Adelaide GV-1	40° 50′	117° 32′	1780	38–107	8	8.1 ±0.8	42.8 ±0.9	3.47 ±0.34	3.32		
				107–305	10	6.80 ±0.62	51.1 ±0.2	3.47 ±0.32	3.41		
				Mean (2 holes)					3.4		
Panther Canyon BM-3	40° 33′	117° 34′	1608	61–160	11	6.81 ±0.38	64.3 ±0.7	4.38 ±0.25		3.5	
BM-37			1635	122–241	13	8.32 ±0.58	57.6 ±1.2	4.79 ±0.25		4.0	
				Mean (2 holes)					3.8		
Elder Creek EC-4	40° 41′	117° 04′	1510	26–252	7	9.5 ±1.1	35.06 ±0.06	3.33 ±0.39	3.2		
Buckingham B-6	40° 37′	117° 04′	1780	61–247	8	8.8 ±1.3	33.2 ±0.3	2.92 ±0.43	2.8		
B-11			1830	152–311	5	8.7 ±0.6	29.66 ±0.15	2.58 ±0.18	2.5		
				Mean (2 holes)					2.7		
Iron Canyon Hole IC-1	40° 33′	117° 06′	1675	259–1410	46	11.2 ±0.5	31.24 ±0.08	3.50 ±0.16	3.50		

TABLE 8. (continued)

Locality	North Latitude	West Longitude	Elevation, meters	Depth Range, meters	N	K, mcal/cm sec °C	Γ, °C/km	q(unc), HFU	q(corr), HFU Category 1	Category 2	Category 3
Nevada (continued)											
Lander Hole TN-1	40° 20'	116° 43'	1670	61–411	10	11.3 ±1.2	30.6 ±0.3	3.46 ±0.35	3.16		
				442–747	12	14.16 ±1.1	24.35 ±0.06	3.45 ±0.28	3.31		
				747–1218	18	7.82 ±0.28	34.1 ±0.1	2.67 ±0.10	2.63		
				Mean					3.0		
Tenabo Hole TN-2	40° 18'	116° 40'	1525	76–343	9	11.72 ±0.48	30.7 ±0.2	3.59 ±0.15	3.53		
Gold Acres GAP-1	40° 16'	116° 45'	1676	122–177	8	9.16 ±0.55	27.2 ±0.2	2.49 ±0.15	2.5		
Swales Mountain Hole SM-2	40° 57'	116° 01'	1829	122–152	9	6.68 ±0.03	22.2 ±0.04	1.48 ±0.01		1.7	
Washington Hill VC-4	39° 28'	119° 38'	1634	61–134	6	4.91 ±0.23	45.8 ±0.6	2.25 ±0.11	2.1		
Lousetown VC-2	39° 23'	119° 38'	1770	30–108	6	4.00 ±0.12	54.7 ±0.6	2.19 ±0.15		2.0	
VC-3	39° 23'	119° 38'	1800	46–111	8	6.24 ±0.54	62.5 ±1.6	3.90 ±0.35		3.5	
Virginia City C-63	39° 18'	119° 39'	1920	107–151	4	8.1 ±0.6	87.7 ±3.4	7.1 ±0.6		7	
Silver City CV-1	39° 15'	119° 40'	1585	137–320	26	6.62 ±0.16	27.60 ±0.04	1.83 ±0.04	1.81		
				320–389	8	11.54 ±0.87	17.66 ±0.21	2.04 ±0.16	1.95		
				389–476	9	9.8 ±1.1	22.50 ±0.36	2.20 ±0.25		2.14	
				Mean					1.93		
Pine Nut Canyon PN-10	38° 53'	119° 35'	1850	58–88	7	7.24 ±0.72	40.34 ±0.25	2.92 ±0.29		2.6	
				88–104	4	8.72 ±1.3	34.4 ±0.3	3.00 ±0.45		2.6	
PN-19	38° 52'	119° 35'	1890	99–183	12	7.05 ±0.63	36.3 ±0.2	2.56 ±0.23	2.26		
				183–383	16	7.95 ±0.19	32.49 ±0.05	2.58 ±0.06	2.38		
				Best value					2.3		

TABLE 8. (continued)

Locality	North Latitude	West Longitude	Elevation, meters	Depth Range, meters	N	K, mcal/cm sec °C	Γ, °C/km	q(unc), HFU	q(corr), HFU Category 1	Category 2	Category 3
Nevada (continued)											
Yerington											
L-2	38° 55'	119° 04'	1463	137–260	9	8.76† ±0.41	20.52 ±0.31	1.80 ±0.09			
L-7	38° 56'	119° 04'	1460	107–350	24	8.29 ±0.16	22.56 ±0.10	1.87 ±0.04			
L-48	38° 56'	119° 04'	1450	107–411	34	8.06 ±0.27	22.80 ±0.14	1.84 ±0.06	1.84		
				Mean (3 holes)				1.84			
Sand Springs											
PM-1	39° 12'	118° 22'	1633	180–320	8	7.04 ±0.03	22.5 ±0.1	1.58 ±0.01	1.58		
PM-2			1621	180–265	0	6.86	18.8 ±0.2	1.29		1.26	
PM-3			1561	70–250	11	6.87 ±0.15	30.8 ±0.1	2.12 ±0.05	1.69		
USBM-1			1585	90–316	0	6.86	24.7 ±0.1	1.69		1.58	
				Mean (4 holes)‡	143	6.86 ±0.04	(22.9)		1.57		
Eureka											
703	39° 30'	116° 00'	1989	165–189	8	6.02 ±0.22	15.6 ±0.3	0.94 ±0.04	0.88		
608	39° 30'	115° 59'	2115	159–245	14	8.18 ±0.10	7.18 ±0.19	0.59 ±0.02	0.58		
720	39° 29'	115° 59'	2318	61–366	5	9.4 ±1.8	10.7 ±0.7	1.01 ±0.20		1.08	
706	39° 29'	115° 59'	2232	31–183	5	9.6 ±1.1	11.2 ±0.4	1.07 ±0.13		1.13	
713	39° 30'	115° 59'	2139	183–450	8	8.38 ±0.12	6.92 ±0.10	0.58 ±0.01	0.60		
				Mean (5 holes)					0.88		
Monitor Valley											
UCe-3	38° 58'	116° 38'	2165	401–597	9	3.94 ±0.26	51.7 ±0.4	2.04 ±0.13	2.0		
Little Fish Lake Valley											
UCe-12A	38° 55'	116° 20'	2111	228–455	9	2.52 ±0.07	49.9 ±0.6	1.26 ±0.04			

TABLE 8. (continued)

Locality	North Latitude	West Longitude	Elevation, meters	Depth Range, meters	N	K, mcal/cm sec °C	Γ, °C/km	q(unc), HFU	q(corr), HFU Category 1	Category 2	Category 3
Nevada (continued)											
				455–582	4	3.62 ±0.36	42.9 ±2.7	1.55 ±0.18			
				582–697	4	5.09 ±0.21	32.3 ±0.4	1.64 ±0.07			
				Mean					1.4		
UCe-9	38° 49'	116° 27'	2088	154–866	0	3.0§	39.4 ±0.2	1.2		1.2	
UCe-10	38° 41'	116° 28'	1980	150–780	7	2.34 ±0.07	49.0 ±0.5	1.15 ±0.04	1.2		
Little Smoky Valley UCe-14	38° 43'	116° 02'	1902	282–393	3	3.0 ±0.3	38.0 ±0.2	1.14 ±0.11			
				424–449	4	5.5 ±0.2	31.5 ±0.9	1.73 ±0.08			
				Best value							1.5
Patterson Pass PP-2	38° 36'	114° 44'	2250	76–151	6‖	7.72ƒ ±0.20	16.21 ±0.45	1.25 ±0.05		1.25	
PP-3			2260	76–305	21	8.92ƒ ±0.34	13.5 ±0.8	1.20 ±0.08		1.20	
				Mean (2 holes)						1.2	
Luning M-4	38° 29'	118° 12'	1585	30–249	18	8.11 ±0.18	88.2 ±1.5	7.15 ±0.20		7.2	
Pilot Mountains DH-1	38° 19'	117° 52'	1978	76–191	10	6.73ƒ ±0.67	28.07 ±0.16	1.89 ±0.19	1.98		
DH-2			1933	99–332	11	6.91ƒ ±0.20	28.17 ±0.06	1.95 ±0.06	1.92		
DH-3			1940	99–267	10	6.94ƒ ±0.36	28.69 ±0.06	1.99 ±0.10	1.98		
				Mean (3 holes)					1.95		
Ralston Valley UCe-1	38° 34'	116° 56'	2150	198–609	153	7.15 ±0.03	25.58 ±0.08	1.83 ±0.01	1.79		
Hot Creek Valley UCe-18	38° 35'	116° 12'	1757	192–1292	11	3.56 ±0.22	36.8 ±0.2	1.31 ±0.08	1.29		
				1292–1664	14	4.94	25.4	1.25	1.24		

TABLE 8. (continued)

Locality	North Latitude	West Longitude	Elevation, meters	Depth Range, meters	N	K, mcal/cm sec °C	Γ, °C/km	q(unc), HFU	q(corr), HFU		
									Category 1	Category 2	Category 3
Nevada (continued)											
Stone Cabin Valley											
UCe-2	38° 18′	116° 35′	1890	Mean		±0.11	±0.4	±0.03	1.28		
				40–162	6	3.84 ±0.28	45.6 ±0.6	1.75¹ ±0.13			
				202–405	9	4.37 ±0.11	25.20 ±0.07	1.10 ±0.03			
Bristol Range											
ESP-3	38° 06′	114° 36′	2061	Mean						1.3	
				602–762	28	7.13 ±0.24	23.32 ±0.14	1.66 ±0.06	1.74		
ESP-1	38° 04′	114° 36′	2274	30–457	18	10.44 ±0.74	13.54 ±0.48	1.41 ±0.11	1.72		
				549–579	6	7.18 ±0.15	20.98 ±0.23	1.51 ±0.04	1.65		
				Mean (2 holes)					1.72		
Manhattan Gap											
MAN-2	37° 58′	114° 36′	2103	152–191	8	7.97 ±1.12	22.16 ±0.74	1.76 ±0.26	1.71		
				198–305	12	9.54 ±1.03	19.44 ±0.20	1.85 ±0.20	1.87		
				Mean					1.83		
MAN-3	37° 57′	114° 36′	2164	30–274	9	8.66 ±0.51	18.05 ±0.22	1.56 ±0.09	1.67		
				305–404	5	16.80 ±0.42	11.38 ±0.09	1.91 ±0.05	2.00		
				404–456	8	8.7 ±1.2	17.93 ±0.17	1.56 ±0.22	1.62		
				Mean					1.75		
MAN-4	37° 58′	114° 36′	2210	296–414	19	9.31 ±0.52	18.1 ±0.2	1.69 ±0.10	1.80		
MAN-7	37° 58′	114° 35′	2200	152–305**	25	9.29 ±0.33	17.08 ±0.16	1.59 ±0.06	1.69		
				305–389††	13	9.28 ±0.48	17.02 ±0.22	1.58 ±0.08	1.67		
				Mean					1.68		
MAN-9	37° 58′	114° 36′	2260	389–509	15	6.91	21.84	1.51	1.59		

TABLE 8. (*continued*)

Locality	North Latitude	West Longitude	Elevation, meters	Depth Range, meters	N	K, mcal/cm sec °C	Γ, °C/km	q(unc), HFU	q(corr), HFU Category 1	Category 2	Category 3
Nevada (continued)											
Silverpeak											
LC-1	37° 43'	117° 47'		Mean (5 holes)		±0.29	±0.29	±0.07	1.74		
			2118	107–228	18	5.44 ±0.18	38.68 ±0.17	2.10 ±0.07	1.85		
LC-4			2136	172–201	8	5.32 ±0.15	41.47 ±0.48	2.21 ±0.07	1.94		
Goldfield				Mean (2 holes)					1.9		
Hole 1	37° 43'	117° 12'	1771	330–465	14	8.76 ±0.22	30.73 ±0.19	2.69 ±0.07			
Hole 2	37° 45'	117° 11'	1731	146–316	11	5.52 ±0.11	35.71 ±0.20	1.97 ±0.04			
				Mean (2 holes)					2.3‡‡		
Tempiute											
SDH-17A	37° 38'	115° 33'	2128	215–288	6	7.76 ±0.23	12.74 ±0.19	0.99 ±0.03	1.05		
SDH-7	37° 38'	115° 33'	2076	447–507	9	8.10 ±0.95	13.03 ±0.10	1.06 ±0.12	1.13		
SDH-18	37° 39'	115° 33'	1975	182–211	12	8.28 ±0.31	13.19 ±0.30	1.09 ±0.05	1.09		
				Mean					1.1		
Pahute Mesa											
PM-2	37° 21'	116° 34'	1703	457–610	4	2.32 ±0.08	56.8 ±0.6	1.32 ±0.05			
				610–732	3	3.15 ±0.15	48.7 ±0.8	1.53 ±0.08			
				732–792	3	4.40 ±0.18	38.2 ±1.9	1.68 ±0.11			
PM-1	37° 17'	116° 24'	1999	Mean 610–914	4	3.06 ±0.25	28.8 ±0.1	0.88 ±0.07			1.5

TABLE 8. (continued)

Locality	North Latitude	West Longitude	Elevation, meters	Depth Range, meters	N	K, mcal/cm sec °C	Γ, °C/km	q(unc), HFU	q(corr), HFU Category 1	Category 2	Category 3
Nevada (continued)											
Dolomite Hill DOL	37° 11'	116° 12'	1950	914–1219	4	4.83 ±0.44	24.4 ±0.1	1.18 ±0.11			
				Mean						1.0	
Yucca Flat TW-E	37° 03'	116° 00'	1272	152–320	7	11.7 ±0.3	16.40 ±0.11	1.92 ±0.05	1.9		
				213–457	9	1.34 ±0.11	48.2 ±0.7	0.65 ±0.05			
				518–701	11	2.27 ±0.07	33.8 ±0.5	0.77 ±0.03			
				Mean					0.7		
Yucca Mountain TW-6	36° 48'	116° 24'	1011	61–290	4	4.4 ±0.2	35.4 ±0.8	1.56 ±0.08		1.6	
Hampel Hill TW-F	36° 46'	116° 07'	1263	564–808	11	4.42 ±0.18	41.77 ±0.07	1.85 ±0.08	1.81		
Frenchman Flat TW-3	36° 46'	115° 52'	1062	137–350	6	6.5 ±0.5	39.9 ±0.7	2.6 ±0.2	2.2		
Rock Valley TW-5	36° 38'	116° 18'	931	61–244	8	6.3 ±0.4	31.1 ±0.6	1.96 ±0.13	2.0		
Indian Spring Valley TW-4	36° 36'	115° 47'	1060	396–457	3	14.2 ±0.4	15.7 ±0.5	2.23 ±0.09		2.17	
Utah Cedar City											
DE-175	37° 42'	113° 17'	1703	76–206	20	7.88 ±0.26	27.09 ±0.32	2.13 ±0.07	2.13		
DE-163	37° 42'	113° 17'	1703	76–335	42	6.98 ±0.21	28.46 ±0.18	1.99 ±0.06	1.99		
DE-104	37° 42'	113° 19'	1725	76–274	28	7.08 ±0.22	29.07 ±0.22	2.06 ±0.07	2.06		
DE-114	37° 41'	113° 19'	1736	53–320	24	6.72 ±0.29	30.39 ±0.21	2.04 ±0.09	2.04		

TABLE 8. (continued)

Locality	North Latitude	West Longitude	Elevation, meters	Depth Range, meters	N	K, mcal/cm sec °C	Γ, °C/km	q(unc), HFU	q(corr), HFU Category 1	Category 2	Category 3
DE-161	37° 41′	113° 19′	1743	76–366	25	8.93 ±0.48	26.47 ±0.40	2.36 ±0.13	2.36		
DE-105	37° 41′	113° 19′	1744	46–290	34	8.48 ±0.40	25.22 ±0.15	2.14 ±0.10	2.14		
N-6	37° 38′	113° 26′	1810	46–107	10	8.97 ±0.27	24.45 ±0.44	2.19 ±0.08	2.19		
				Best value	29	6.70 ±0.09	(28.06)ⁱ	1.88 ±0.04	1.88		

* Estimated conductivity.
† K from Roy [1963].
‡ All but 19 of the conductivity samples came from nearby holes (<1 km away) in the same material.
§ K is a regional average for 35 samples of the same material.
‖ Samples from PP-3.
¶ Tuffs, above static-water level. If the regional average K (3) is used, q(unc) is 1.4.
** Temperatures measured in air.
†† Temperatures measured in water.
‡‡ A combination of conductivity structure and sampling bias resulted in an overestimate of q(unc) in hole 1, and an underestimate in hole 2.

conductivities in that particular data set were measured on fragments or by the needle probe, respectively (see section on conductivity, above).

The gradient Γ (column 8) is represented in three different ways, depending on which of the following methods of heat-flow reduction was used:

1. If there was conductivity stratification on a scale of 50 meters or larger, one line of the table is devoted to each stratum. Γ is the least-square temperature gradient (± standard error) over the depth range indicated (column 5), and the uncorrected heat flow q(unc), column 9, is the product of this gradient and the mean conductivity (column 7).

2. If conductivity stratification was on a smaller scale, then the heat flow for each of the layers is determined as in 1, and their weighted mean for the depth range indicated (column 5) is entered in column 9. For consistency, the arithmetic mean conductivity (and its standard error) for the entire depth range is entered in column 7, and the gradient consistent with that conductivity and the heat flow (column 9) is entered in column 8. This derived gradient is shown in parentheses with a superscript i (for interval method).

3. In inhomogeneous materials in which the conductivity stratification is not clearly defined, the resistance integral technique of Bullard [1939] was used to determine q(unc). As in method 2, a derived gradient consistent with K (column 7) and q(unc) (column 9) is entered in parentheses in column 8. The gradient entry has the superscript b (for Bullard method).

The final three columns headed q(corr) represent the best estimate of heat flow with corrections where appropriate and category assignments according to criteria outlined above. In the majority of cases if a correction was applied, it was for steady-state topography, but estimates of other sources of disturbance were sometimes made in evaluating a heat flow and assigning it to a category. As stated in the introduction, detailed documentation for each of the heat-flow determinations in Tables 1 through 8 is in preparation.

In areas where there were two or more holes within a small area (~10 km²), a single value is given below all the others, representing the best estimate of the heat flow in the area. This is generally the mean (weighted by the length of the applicable depth interval) of all holes, but this can be altered by local factors. For example, the average q from eight holes near Cedar City, Utah (see Table 8), is about 2.1. There is, however, a strong suggestion of sampling bias toward silicic rocks in some of the heterogeneous sedimentary formations. Sampling was not a problem in the Homestake limestone, a dense, marine limestone formation. Here, 24 component heat flows calculated by the interval method were tightly grouped about a mean of 1.88 ± 0.04, and this value was adopted for the area.

DISCUSSION

The foregoing tables contain about 150 new heat-flow determinations representing roughly 100 distinct sites separated from one another by at least a few kilometers. As this more than doubles the published heat-flow data from the western United States, it is worth looking briefly at the present status of the observations. Interpretive studies of these data and additional results being obtained in such key areas as the Klamath Mountains are under way, and they will be reported separately.

Figure 3 distinguishes between the locations of heat flows reported herein (squares) and those previously published (triangles). Figure 4 distinguishes between all heat flows with values in the 'low-to-normal' range (defined by q ≤ 1.5 HFU) and those 'higher than normal' (defined by q ≥ 1.6 HFU, with all values rounded to the nearest 0.1 HFU). It is seen from Figure 3 that the western United States as a whole is still very poorly sampled. From Figure 4 and the histogram, Figure 5, it is seen that the heat flow as we now know it is extremely variable and is dominated by higher-than-normal values. That part of the western United States to the west of the Great Plains corresponds to the 'Mesozoic-Cenozoic orogenic areas' of Lee and Uyeda [1965]. The most recent compilation of 159 values from such areas throughout the world [Lee, 1970] yielded a mean of 1.76 and standard deviation of 0.58. These values are almost identical to those shown for the western United States in Figure 5. This tends to confirm Lee's results even
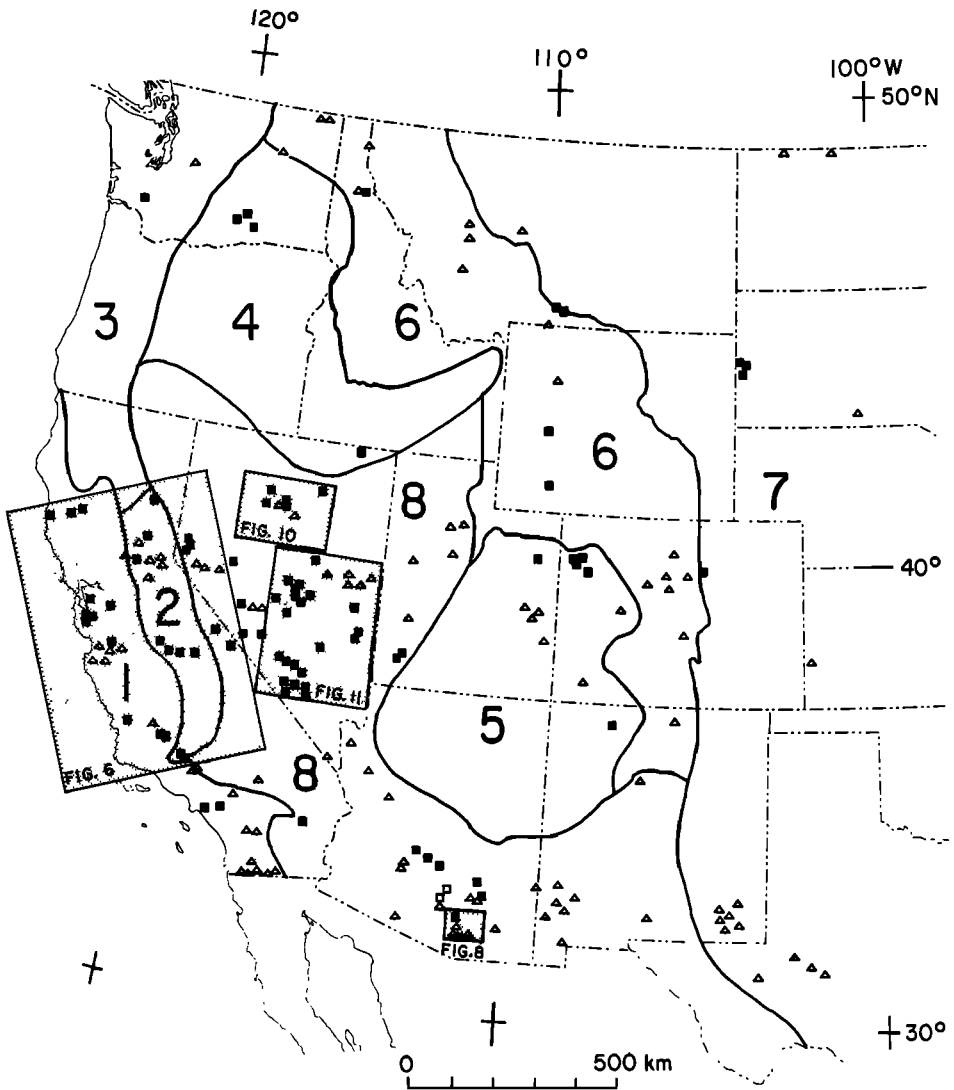
Fig. 3. Sketch map of the western United States showing the locations of heat-flow measurements: Triangles, previously published data (see text for references); squares, U.S. Geological Survey data. The stippled rectangles are shown in greater detail in Figures 6, 8, 10, and 11. The numbers refer to the same physiographic provinces in the corresponding tables.
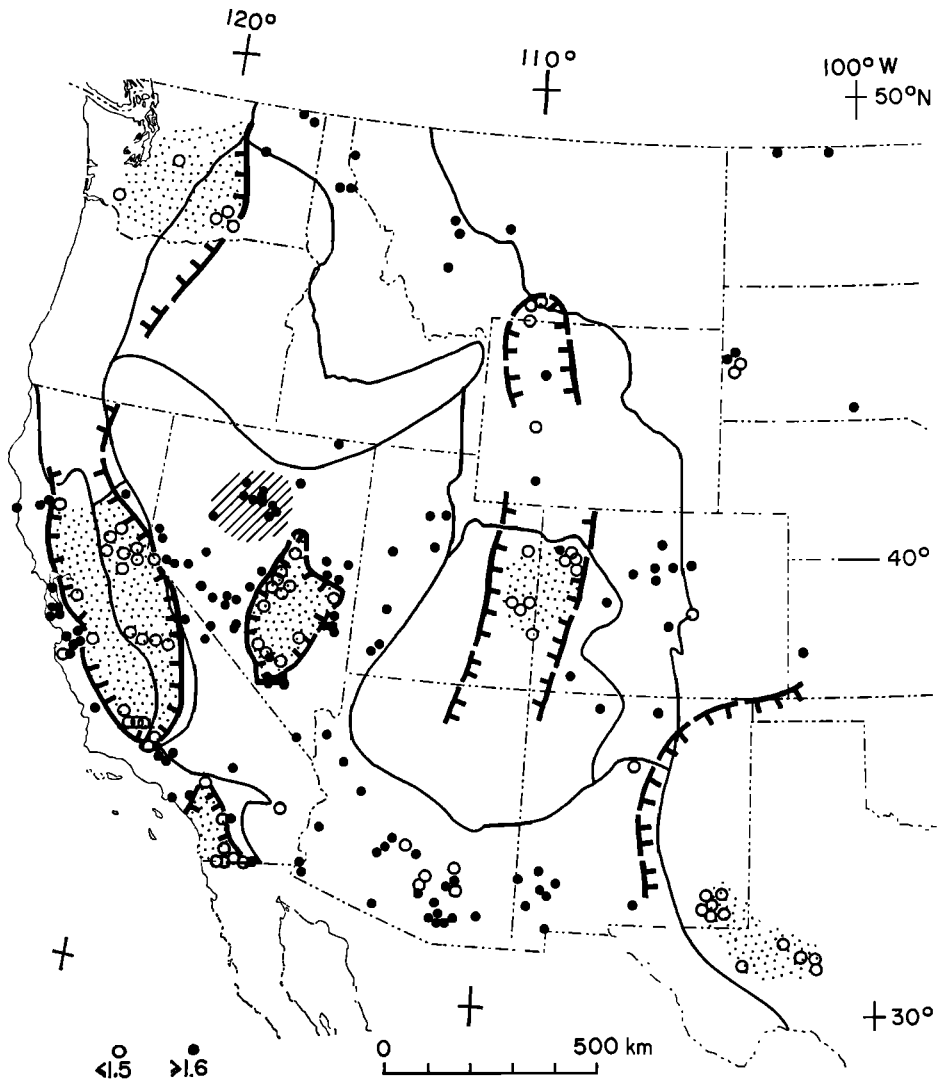
Fig. 4. Generalized representation of heat-flow data from the western United States. Stippled areas are characterized by heat flows of 1.5 and less; the heavy lines are 1.5 HFU contours. The cross-hatched area is characterized by heat flow of 2.5 and greater.
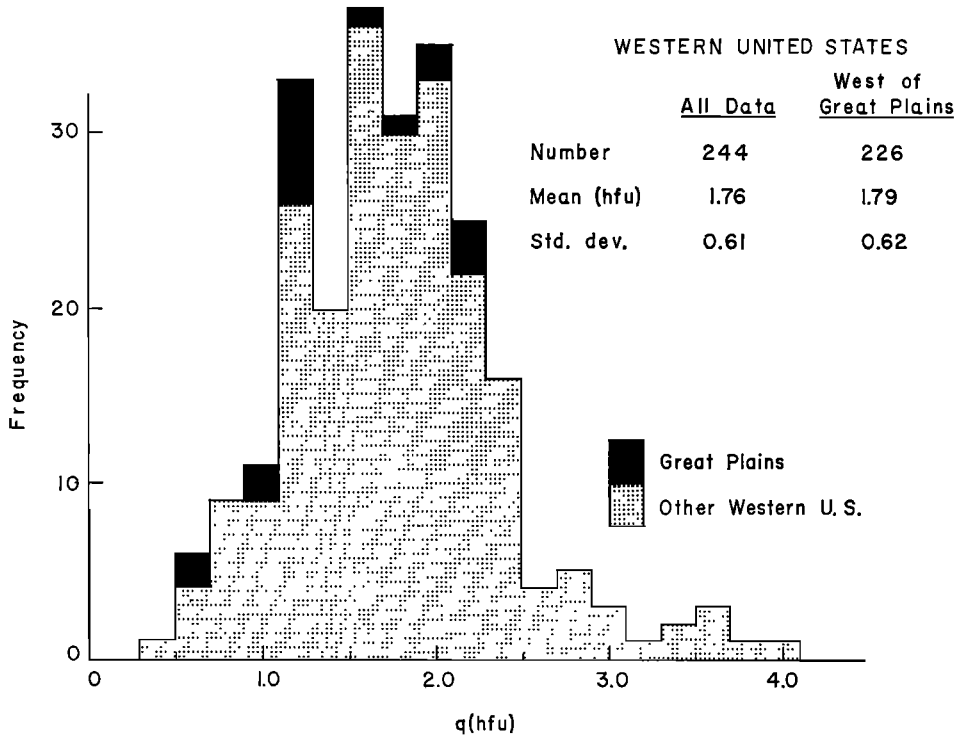
Fig. 5. Histogram of all heat-flow determinations in the western United States. Values greater than 4 HFU were omitted from the analysis.

though almost 100 values are common to both analyses.

From the simple binary division of heat-flow values in Figure 4, it is clear that heat flow from the western United States need not be treated as a homogeneous population. This fact has, of course, been recognized for some time, and many of the features in Figure 4 have been identified by *Roy et al.* [1971] from previously published data. Although the predominant heat flow in the western United States seems to be higher than normal, several regions of lower heat flow with lateral dimensions an order of magnitude greater than crustal thickness can be identified (stippled areas, Figure 4). The heavy dashed lines enclosing these regions (Figure 4) represent a preliminary interpretation of the 1.5 HFU contour. (It is of some interest to note the general coincidence of this contour and the lines enclosing the region of intermediate crustal seismic velocity in Figure 2, *Pakiser and Zietz* [1965].) More refined contouring is probably warranted only in

the Sierra Nevada–Great Valley–Coast Range area of California shown in Figure 6.

The semicontinuous band of lower heat flows paralleling the west coast and its gross relation to the San Andreas transform fault system in California suggest explanations in terms of lithospheric subduction and related tectonic processes [see e.g., *Blackwell and Roy*, 1971; *Roy et al.*, 1971]. These models are sensitive to assumptions regarding the magnitudes and distribution in time and space of the opposing effects of cooling by descending plates and heating by friction, compression, radioactivity, and ascending melts. Our present ignorance of the mechanics of these processes permits a broad range of assumptions and a wide variety of explanations of the heat-flow pattern. It is hoped that work in progress at several institutions will increase the heat-flow coverage of this region sufficiently to obtain more useful constraints for models of the continental margin.

One region of conspicuously high heat flow
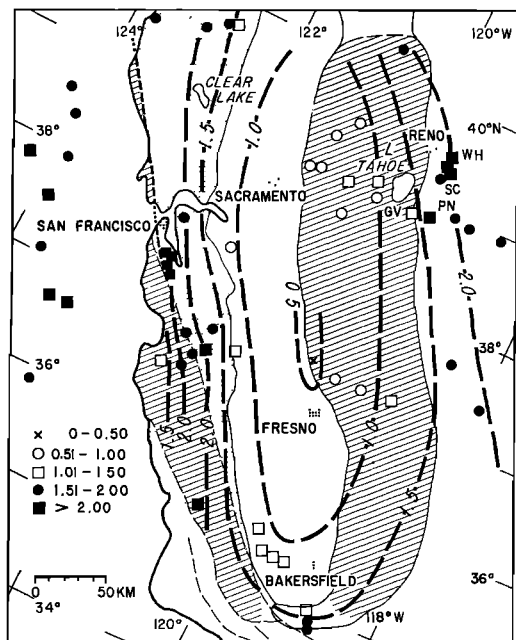
Fig. 6. Heat-flow values in central California and western-central Nevada. (See Figure 3 for location.) Contour interval, 0.5 HFU. The offshore measurements are from *Foster* [1962] and *Burns and Grim* [1967]. The strippled area is the Franciscan block; shaded areas, the Sierra Nevada and Salinian blocks.

occurs in north-central Nevada (cross hatching, Figure 4). The boundaries of this region, and possibly others as yet undetected, could be delineated by more systematic heat-flow coverage. This could provide useful guidance in the search for economically exploitable geothermal fields.

Some comments on the status of observations in the individual provinces follow.

California coastal province (Table 1). This province includes such diverse physiographic regions as the great Central Valley, the Coast Ranges, the peninsular ranges, and the Los Angeles basin. The range of heat flow reflects the heterogeneity of the province.

Heat flow is high in the Franciscan terrane in the vicinity of San Francisco Bay, where all values are around 2.0, irrespective of distance from the major strike-slip faults. This is consistent with measurements farther south by *Brune et al.* [1969], and *Henyey* [1968], which showed no significant heat-flow anomalies associated with strike-slip faults in California.

The numerous hot springs in the Coast Ranges north of the San Francisco Bay area up to Clear Lake at about latitude 39°N [*Waring*, 1965] indicate that the band of high heat flow extends northwestward at least that far. North of Clear Lake, heat flow seems high near the coast but decreases inland to a normal value near the eastern limit of Franciscan rocks (Figure 6). The measurements along the western margin of the Central Valley are low to normal, consistent with the earlier result of *Benfield* [1947] near Bakersfield. Measurements in the Los Angeles basin and near Santa Ana indicate a region of high heat flow there (Figure 4).

Sierra Nevada (Table 2). With seven measurements less than 0.75 HFU, the western margin of the Sierra Nevada is now one of the best documented areas of low heat flow on the continents. This finding came as a surprise to many because of the observed masses of granite that were thought to contain sufficient heat sources to account for much higher heat flows. It is consistent, however, with low values reported from the ocean side of circum-Pacific granitic rocks in Chile [*Diment et al.*, 1965], Amchitka Island [*Sass and Munroe*, 1970], and northeastern Honshu Island [*Uyeda and Horai*, 1964] in what might be related tectonic settings. Theoretical considerations indicate that the paradox results primarily from anomalously low heat flow from the mantle underlying the Sierra Nevada province and secondarily from the low heat production of granitic rocks in the western part of the Sierra [*Roy et al.*, 1968b; *Lachenbruch*, 1968a, 1970]. It now appears that the mantle (or deep crustal) heat flow in the Sierra (0.4 HFU) is only about half that characteristic of stable regions and less than one-third that of the Basin and Range province to the east. The increase in heat flow eastward to the Sierra crest (Figure 6) seems generally to correspond to an increase in crustal heat production. The transition at the Basin and Range boundary is discussed in a later paragraph.

Physiographically, the Tehachapi Mountains are the southern 'toe' of the Sierra Nevada. They are, however, different from the Sierra with respect to structure, origin, and geological history [*Bulwalda*, 1954].

Many holes were drilled by the California Division of Water Resources along the pro-

posed route for the California aqueduct system. Suitable temperatures were measured in four of the holes, and heat flows are listed in Table 2b. For DH 43 and DH 65, the heat flows are in reasonable agreement with later measurements in the same holes by *Henyey* [1968]. The Tehachapi range appears to provide a thermal as well as a physiographic boundary between the San Joaquin Valley (low-to-normal heat flow) and the Mojave block of the Basin and Range province, which is probably characterized by higher-than-normal heat flow (Figures 4 and 6).

Pacific Northwest coastal province. Table 3 presents one of the first reliable estimates of heat flow from this province. This low value near Chehalis, Washington, raises the possibility that the crustal heat production in the area is low or, alternatively, that this province is similar to the Sierra Nevada, having a very low heat flow from the mantle. Intrusive rocks were not encountered at Chehalis, and they are rare in the area. Where Tertiary intrusive rocks are seen, they are mafic sills of gabbro or basalt porphyry [see e.g., *Snavely et al.*, 1958; *Henriksen*, 1956]. H. C. Wagner and P. D. Snavely, Jr., reported in 1966 that the pre-Tertiary crystalline basement of western Washington (not exposed in the Chehalis area) is principally gneissic amphibolite and quartz diorite (in unpublished report of U.S. Congressional Committee on Interior and Insular Affairs, 89th Congress, 2nd Session, pp. 37–46). Thus the small amount of information available on deep crustal composition indicates a rather mafic crust containing few radiogenic heat sources, an observation consistent with the low observed heat flow and a moderate heat flow from the mantle.

Columbia Plateaus. Largely on the basis of observed volcanism, hot spring activity, and seismicity, *Blackwell* [1969] included the Columbia Plateau in his postulated 'Cordilleran Thermal Anomaly Zone' (CTAZ) of high heat flow. From the present results (Table 4) it appears that at least the western part of the plateaus may be part of a province of low-to-normal heat flow (see also Figure 4). A single high value from northeastern Nevada supports the assumption that the Snake River Plain is part of the CTAZ (Figure 4).

The Colorado Plateau (Table 5). A heat flow of 2.01 was obtained near the eastern boundary of the plateau. This high value is consistent with the findings of *Decker* [1969, and personal communication] in this part of the plateau and the neighboring southern Rocky Mountains, and with the suggestion [*Edwards*, 1966] that this part of the plateau is underlain by granitic rocks. In the northern part of the plateau, five new sites give normal values with only one (category 3) value as high as 2 (Figures 3 and 4). This part of the plateau evidently is underlain by a Precambrian sedimentary terrane [*Edwards*, 1966]. Low heat flow in the northern Colorado Plateau is also consistent with *Porath's* [1971] interpretation of the depth to an electrically conductive layer in this region on the basis of observed magnetic variation anomalies.

Rocky Mountain province (Table 6). A value of 2.3 was measured in the Galena mine near Wallace, Idaho, confirming the high values measured by *Blackwell* [1969] slightly to the east. The five estimates of heat flow from the central Rocky Mountains are all in the range 1.3 to 1.6 HFU. The high value measured at Denver is included in the Rocky Mountains even though Denver is physiographically part of the Great Plains. This is higher than the nearest neigboring point, *Decker's* [1969] value of 1.52 at Golden, but it is consistent with the general pattern of high heat flow in the southern Rocky Mountains.

Great Plains province (Table 7). The only heat-flow estimates made in the Great Plains during this work were at three sites in the Black Hills of South Dakota and one near Lyons, Kansas (not shown in Figures 3 and 4). The Black Hills values show a very large variation over a relatively small area, and none is in category 1. The hole at Dacy (which agrees with *Blackwell's* [1969] estimate at Lead) had been completed only 10 days before the temperature measurements were made, and there was evidence of residual drilling disturbances in the temperature profile. Water was flowing slowly but steadily from the collars of both holes from which heat flow is low. Examination of the temperature profiles (Figure 7), however, indicated no vertical water movement below the zone of influx of the Artesian flow, and the vertical temperature profiles below these points were linear and mutually consistent. The

low heat flows may well be the result of some fairly deep seated regional hydrologic effect of long duration that has, in effect, thermally decoupled the rocks penetrated by these holes from the earth below. On the other hand, the possibility that the high heat flows at Lead and Dacy are the result of some local anomalous situation cannot be ignored. We do not have enough information to define a regional heat flow for the Black Hills.

Basin and Range province (Table 8). The majority of the data presented in this paper are from the Basin and Range physiographic province, and they generally confirm that this province is one of high heat flow (Figure 4). In addition, however, the new data define some distinct subprovinces, and they place further constraints on the nature of the transition between the Sierra Nevada and the Basin and Range provinces.

Tucson area. A detailed examination of the 15 heat-flow determinations in a 100 km² area near Tucson serves to illustrate some of the problems of measuring heat flow in the Basin and Range province and to emphasize that even a 'first-rate' single determination in a region of unknown, complicated structure can be a poor indicator of the actual regional heat flux.

Our six values in this region are all in category 1, and, from the information given in their table, it appears that all the values of *Roy et al.* [1968*b*] are also in this category. There is, however, a spread of nearly a factor of 2 between the extreme values (Figures 8 and 9 and Table 9). Despite the variation within each set of determinations, the mean heat flow determined from one set is not significantly different from that calculated from the other (see Table 9).

The structural complexity and the range of heat-flow values encountered in this region are similar to those encountered at Mt. Isa, Queensland, by *Hyndman and Sass* [1966]. In the present instance, even though the general structure of the region is well known from drilling and mining operations, there is insufficient knowledge of detailed structure to make the necessary corrections. The combination of steeply dipping beds of contrasting conductivity and ubiquitous faults on every scale probably results in a 'worst case' situation in this region, and several holes are needed to arrive at a re-
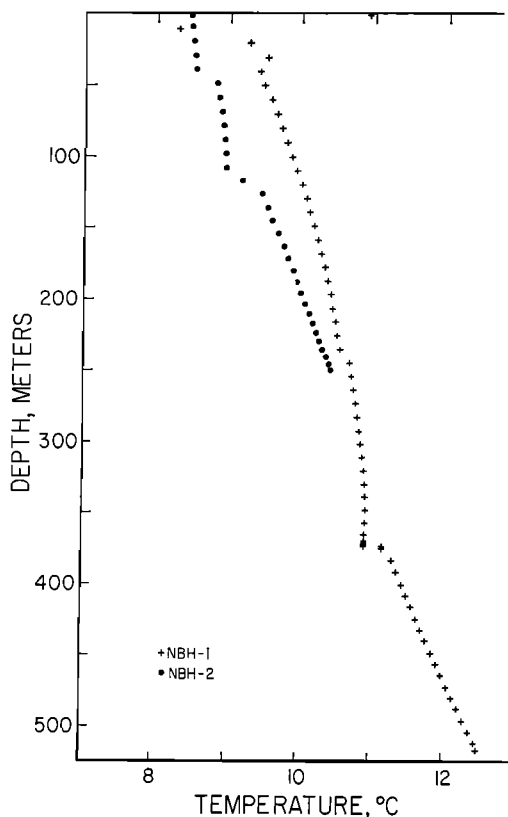
Fig. 7. Temperature profiles from Windy flats (NBH-1) and Moonshine gulch (NBH-2), South Dakota. See Table 7.

liable estimate of regional heat flux. The coefficient of correlation between q and K is about 0.23 (Figure 9), a value typical of many found by *Horai and Nur* [1970] on a larger scale. This poor correlation implies a complicated situation that cannot be resolved by simple geometrical refraction models even on a scale as small as that illustrated in Figure 8.

Subprovinces in the Basin and Range. Most heat-flow values in this province are in the range 1.5 to 2.5 HFU. There are some isolated very high and low-to-normal values that are most probably related to local hydrologic conditions. In addition, however, there are clusters of consistently high or low values of regional extent for which we must seek more deepseated causes. From the present work, we define the 'Battle Mountain high' (Figure 10) and the 'Eureka low' (Figure 11). There is also a single category-1 datum of 1.3 HFU near Eagle
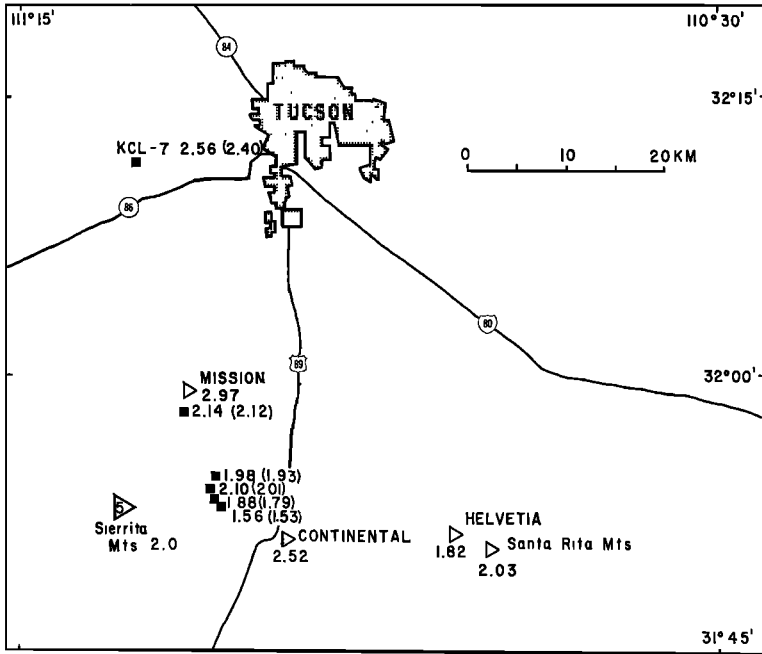
Fig. 8. Heat flows near Tucson, Arizona (see Figure 3 for location). Triangles, values from *Roy et al.* [1968b]; squares, U.S. Geological Survey values. The values in parentheses were calculated in the same way as those of Roy et al.
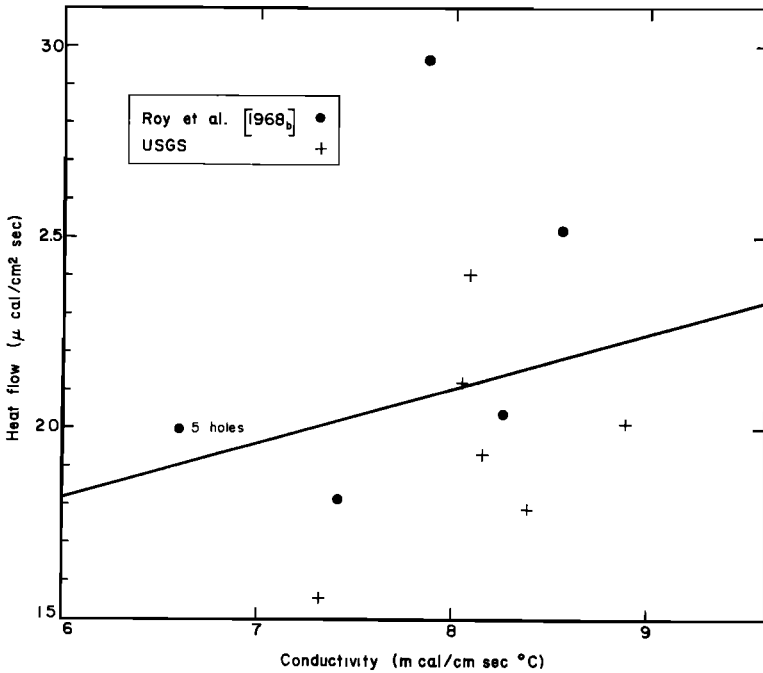
Fig. 9. Heat flow versus mean conductivity for the locations shown in Figure 8.

TABLE 9. Mean Heat Flows in HFU for the Region South and West of Tucson, Arizona
(Range of individual values, 1.56 to 2.97)

Source of Data	Number of Holes	Total Length,* meters	Average Heat Flow	Standard Error
Present work	6	1400	2.04	0.13
Roy et al. [1968*b*]	9	1430	2.15	0.12
Present work and *Roy et al.* [1968*b*]	15	2830	2.10†	0.09
Present work and *Roy et al.* [1968*b*]	15	2830	2.12‡	0.06

* This includes only those parts of the holes for which temperatures were used to calculate heat flow.
† Simple average of all values.
‡ Mean weighted according to the length of individual holes.

Mountain, California (in the Mojave Block), which may form part of a region of normal heat flow.

It is interesting that there are no thermal springs near Eagle Mountain and that within the Eureka low the thermal springs are less common and are cooler than in the surrounding areas [see *Waring*, 1965]. By contrast, the Battle Mountain high contains a fairly dense, regular distribution of warm-to-hot–water springs including the well-known Beowawe geysers (Figure 10).

The high mean heat flow from the Basin and Range province has been interpreted in terms of near-melting conditions in the lower crust and upper mantle [see e.g. *Roy and Blackwell*, 1966; *Roy et al.*, 1968*b*, 1971; *Lachenbruch*, 1970], and it seems reasonable to interpret the Battle Mountain high as a transient effect of fairly recent crustal intrusion. This view is supported by evidence of Quaternary volcanism within the region [see e.g., *Roberts*, 1964].

Figure 11 shows a large area north of Las Vegas, which we have called the 'Eureka low,' characterized by heat flows in the range of 0.7 to 1.5 HFU. (The relatively high value of 1.9
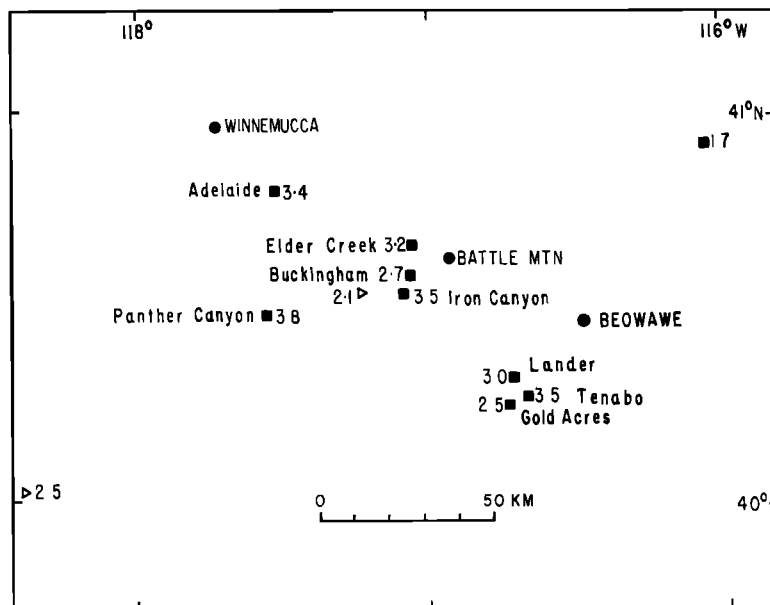
Fig. 10. Heat flows within the 'Battle Mountain high' (see Figure 3 for location). The symbols are as in Figure 8.
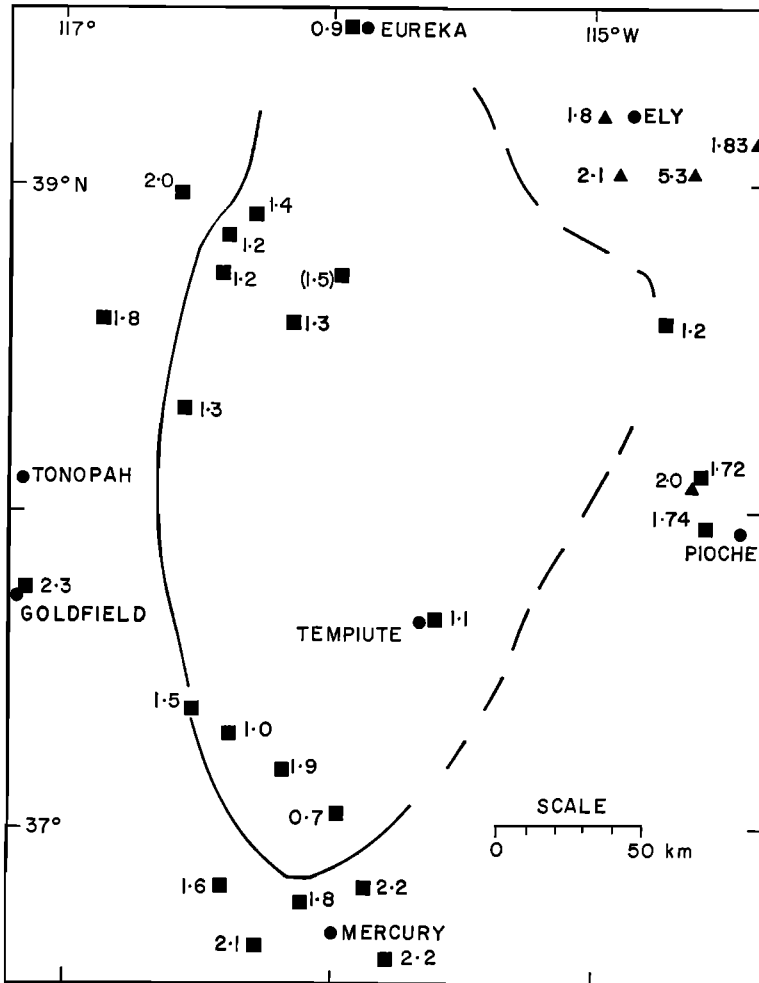
Fig. 11. Heat flows between Mercury and Eureka, Nevada (see Figure 3 for location); the heavy line is a 1.5-HFU contour defining the 'Eureka low.' Symbols are as in Figure 8.

near the southern end of the Eureka low was measured in dolomite near a contact with volcanic rocks and may be caused, in part, by refraction.) This large apparent anomaly in the normally 'hot' Basin and Range may be interpreted in at least two ways. It could represent a systematic hydrologic effect of regional extent or it might be a region where temperatures in the lower crust and upper mantle have been below the solidus for some time. However, the abrupt transitions on the margin of the feature (Figure 11) favor a fairly shallow origin for the anomaly. Our fragmentary temperature data from very deep holes in southern Nevada suggest an explanation in terms of

systematic though complex interbasin ground water flow with appreciable vertical velocity components to depths of about 3 km (~1 km below sea level). The identification of such flow patterns is, of course, fundamental to an understanding of the hydrology of this large arid area [see e.g. *Winograd and Thordarson*, 1968]. It is also fundamental to the evaluation of regional heat-flow analyses, since the conductive flux determined in the upper kilometer is usually identified tacitly with heat loss from the earth's interior. It is seen (Table 8) that several heat flows in the Eureka low have been assigned to the 'highest quality' category (1) on the basis of usually applied criteria of in-

ternal consistency. Only under exceptional circumstances will supplementary information be available to reveal the possible occurrence of deep-seated 'hydrologic decoupling' on a regional scale.

The Sierra Nevada–Basin and Range transition. Roy and Blackwell [1966] and *Roy et al.* [1968*b*, 1971] have concluded that the transition between these two provinces takes place over a short distance (on the order of 100 km) within the Basin and Range province. Data now available suggest a more abrupt transition that might extend into the eastern Sierra Nevada.

Figure 6 shows all the previously published data along the transition together with the present results. The most striking increase in heat flow is that between Gardnerville (GV) and the Pine Nut Canyon (PN). If equal weight is given to the two values, then we must conclude that the transition occurs within 20 km. North of these points the new data firmly establish high heat flow between Carson City and Reno, only 15 to 20 km from the physiographic boundary of the Sierra province. Although independent evidence [*Becker*, 1882] indicates that the very high heat flows near the Comstock lode are from local hydrologic effects, no such effects are evident at Washington Hill (WH), Silver City (SC), or Pine Nut Canyon (PN) (Figure 6). Measurements at Black Rock and Deep Spring 150 km to the south, (10 and 35 km from the physiographic boundary), also indicate high heat flow extending very close to the edge of the Basin and Range province.

As previously mentioned, interpretive studies suggest that the thermal transition from the Basin and Range province to the Sierra Nevada might involve a change in heat flow from the deep crust or mantle by a factor of 3. Such a transition would be extremely difficult to explain by almost any model if it occurred over a lateral distance of only 10 or 20 km (a situation that must exist if we assume that the transition zone is in the Basin and Range province). It therefore seems probable that, like the Basin and Range faulting, the heat-flow transition extends into the eastern Sierra. This view is supported by recent heat-flow results from Lake Tahoe presented by *Lee and Henyey* [1970].

REFERENCES

Beck, A. E., Techniques of measuring heat flow on land, in *Terrestrial Heat Flow, Geophys. Monogr. Ser.*, vol. 8, edited by W. H. K. Lee, pp. 24–57, AGU, Washington, D. C., 1965.

Becker, G. F., *Geology of the Comstock Lode and the Washoe District, U.S. Geol. Surv. Monogr. 3*, 422 pp., 1882.

Benfield, A. E., A heat flow value for a well in California, *Amer. J. Sci., 245*, 1–18, 1947.

Birch, Francis, Temperature and heat flow in a well near Colorado Springs, *Amer. J. Sci., 245*, 733–753, 1947.

Birch, Francis, The effects of Pleistocene climatic variations upon geothermal gradients, *Amer. J. Sci., 246*, 729–760, 1948.

Birch, Francis, Flow of heat in the Front Range, Colorado, *Geol. Soc. Amer. Bull., 61*, 567–630, 1950.

Birch, Francis, The present state of geothermal investigations, *Geophysics, 19*, 645-659, 1954.

Birch, Francis, and Harry Clark, The thermal conductivity of rocks and its dependence on temperature and composition, *Amer. J. Sci., 238*, 529–558 and 613–635, 1940.

Birch, Francis, R. F. Roy, and E. R. Decker, Heat flow and thermal history in New England and New York, in *Studies of Appalachian Geology: Northern and Maritime*, edited by E-an Zen, W. S. White, J. B. Hadley, and J. B. Thompson. Jr., pp. 437–451, Interscience, New York, 1968.

Blackwell, D. D., Heat-flow determinations in the northwestern United States, *J. Geophys. Res., 74*, 992–1007, 1969.

Blackwell, D. D., and R. F. Roy, Geotectonics and Cenozoic history of the western United States (abstract), *Geol. Soc. America, Cordil-*

leran Sect., 67th Annu. Meet., Riverside, Calif., 1971, Abstr. Programs, 3, 84–85, 1971.

Bredehoeft J. D., and I. S. Papadopulos, Rates of vertical groundwater movement estimated from the earth's thermal profile, Water Resour. Res., 1, 325–328, 1965.

Brune, J. N., T. L. Henyey, and R. F. Roy, Heat flow, stress, and rate of slip along the San Andreas fault, California, J. Geophys. Res., 74, 3821–3827, 1969.

Bullard, E. C., Heat flow in South Africa, Proc. Roy. Soc. London, Ser. A, 173, 474–502, 1939.

Bullard, E. C., The time necessary for a borehole to attain temperature equilibrium, Mon. Not. Roy. Astron. Soc., Geophys. Suppl., 5, 127–130, 1947.

Burns, R. E., and P. J. Grim, Heat flow in the Pacific Ocean off central California, J. Geophys. Res., 72, 6239–6247, 1967.

Buwalda, J. P., Geology of the Tehachapi Mountains, California, in Geology of Southern California, edited by R. H. Jahns, Calif. Dep. Natur. Resour. Div. Mines Bull., 170(6), 131–142, 1934.

Clark, S. P., Jr., Heat flow at Grass Valley, California, Eos Trans. AGU, 38, 239–244, 1957.

Combs, J. B., Terrestrial heat flow in north central United States, Ph.D. thesis, Massachusetts Institute of Technology, Cambridge, 1970.

Costain, J. K., and P. M. Wright, Heat flow and geothermal measurements in Utah (abstract), Eos Trans. AGU, 49, 325, 1968.

Decker, E. R., Heat flow in Colorado and New Mexico, J. Geophys. Res., 74, 550–559, 1969.

Diment, W. H., Francisco Ortiz O., Louis Silva R., and Carlos Ruiz F., Terrestrial heat flow at two localities near Vallenar, Chile (abstract), Eos Trans. AGU, 46, 175, 1965.

Edwards, Jonathan, Jr., The petrology and structure of the buried Precambrian basement of Colorado, Quart. Colo. School Mines, 61(4), 436 pp., 1966.

Fenneman, N. M., Physiographic divisions of the United States, Ann. Ass. Amer. Geogr., 18, 261–353, 1928.

Foster, T. D., Heat-flow measurements in the northeast Pacific and in the Bering Sea, J. Geophys. Res., 67, 2991–2993, 1962.

Henriksen, D. A., Eocene stratigraphy of the lower Cowlitz River-eastern Willapa Hills area, southwestern Washington, Wash. Dep. Conserv. Div. Mines Geol. Bull., 43, 122 pp., 1956.

Henyey, T. L., Heat flow near major strike-slip faults in central and southern California, Ph.D. thesis, California Institute of Technology, Pasadena, 1968.

Herrin, Eugene, and S. P. Clark, Jr., Heat flow in west Texas and eastern New Mexico, Geophysics, 21, 1087–1099, 1956.

Horai, Ki-iti, and Amos Nur, Relationship among terrestrial heat flow, thermal conductivity, and geothermal gradient, J. Geophys. Res., 75, 1985–1991, 1970.

Howard, L. E., and J. H. Sass, Terrestrial heat flow in Australia, J. Geophys. Res., 69, 299–308, 1964.

Hyndman, R. D., and J. H. Sass, Geothermal measurements at Mount Isa, Queensland, J. Geophys. Res., 71, 587–601, 1966.

Jaeger, J. C., The effect of the drilling fluid on temperatures measured in boreholes, J. Geophys. Res., 66, 563–569, 1961.

Jaeger, J. C., Application of the theory of heat conduction to geothermal measurements, in Terrestrial Heat Flow, Geophys. Monogr. Ser., vol. 8, edited by W. H. K. Lee, pp. 7–23, AGU, Washington, D. C., 1965.

Jaeger, J. C., and J. H. Sass, Lee's topographic correction in heat flow and the geothermal flux in Tasmania, Geofis. Pura Appl., 54, 53–63, 1963.

Jaeger, J. C., and R. F. Thyer, Report on progress in geophysics: Geophysics in Australia, Geophys. J., 3, 450–461, 1960.

Kraskovski, S. A., On the thermal field in shields, Izv. Akad. Nauk. SSSR, Ser. Geofiz., 247–250, 1961.

Lachenbruch, A. H., Three-dimensional heat flow in permafrost beneath heated buildings, U.S. Geol. Surv. Bull. 1052-B, 51–69, 1957a.

Lachenbruch, A. H., Thermal effects of the ocean on permafrost, Geol. Soc. Amer. Bull., 68, 1515–1529, 1957b.

Lachenbruch, A. H., Preliminary geothermal model of the Sierra Nevada, J. Geophys. Res., 73, 6977–6989, 1968a.

Lachenbruch, A. H., Rapid estimation of the topographic disturbance to superficial thermal gradients, Rev. Geophys. Space Phys., 6, 365–400, 1968b.

Lachenbruch, A. H., Crustal temperature and heat production: Implications of the linear heat-flow relation, J. Geophys. Res., 75, 3291–3300, 1970.

Lachenbruch, A. H., and M. C. Brewer, Dissipation of the temperature effect of drilling a well in arctic Alaska, U.S. Geol. Surv. Bull. 1083-C, 73–109, 1959.

Lachenbruch, A. H., and B. V. Marshall, Heat flow through the Arctic Ocean floor: The Canada basin-Alpha rise boundary, J. Geophys. Res., 71, 1223–1248, 1966.

Lachenbruch, A. H., and B. V. Marshall, Heat flow in the Arctic, Arctic, 22, 300–311, 1969.

Lachenbruch, A. H., M. C. Brewer, G. W. Greene, and B. V. Marshall, Temperatures in permafrost, in Temperature—Its Measurement and Control in Science and Industry, edited by C. M. Herzfeld, vol. 3, pp. 791–803, Reinhold, New York, 1962.

Lachenbruch, A. H., H. A. Wollenberg, G. W. Greene, and A. R. Smith, Heat flow and heat production in the central Sierra Nevada, preliminary results (abstract), Eos Trans. AGU, 47, 179, 1966.

Lee, T. C., and T. L. Henyey, Heat flow in Lake Tahoe, California-Nevada (abstract), Eos Trans. AGU, 51, 824, 1970.

Lee, W. H. K., On the global variation of terres-

trial heat flow, *Phys. Earth Planet. Interiors, 2,* 332–341, 1970.

Lee, W. H. K., and Seiya Uyeda, Review of heat flow data, in *Terrestrial Heat Flow, Geophys. Monogr. Ser., vol. 8,* edited by W. H. K. Lee, pp. 87–190, AGU, Washington, D. C., 1965.

Pakiser, L. C., and Isidore Zietz, Transcontinental crustal and uppermantle structure, *Rev. Geophys. Space Phys., 3,* 505, 1965.

Porath, H., Magnetic variation anomalies and seismic low-velocity zone in the western United States, *J. Geophys. Res., 76,* 2643, 1971.

Ratcliffe, E. H., Thermal conductivities of fused and crystalline quartz, *Brit. J. Appl. Phys., 10,* 22–28, 1959.

Roberts, R. J., Stratigraphy and structure of the Antler Peak quadrangle, Humboldt and Lander counties, Nevada, *U.S. Geol. Surv. Prof. Pap. 459-A,* A1–A93, 1964.

Roy, R. F., Heat flow measurements in the United States, Ph.D. thesis, Harvard University, Cambridge, Mass., 1963.

Roy, R. F., and D. D. Blackwell, Heat flow in the Sierra Nevada and western Great Basin (abstract), *Eos Trans. AGU, 47,* 179–180, 1966.

Roy, R. F., D. D. Blackwell, and Francis Birch, Heat generation of plutonic rocks and continental heat flow provinces, *Earth Planet. Sci. Lett., 5,* 1–12, 1968a.

Roy, R. F., E. R. Decker, D. D. Blackwell, and Francis Birch, Heat flow in the United States, *J. Geophys. Res., 733,* 5207–5221, 1968b.

Roy, R. F., D. D. Blackwell, and E. R. Decker, Continental heat flow, in *The Nature of the Solid Earth,* edited by E. C. Robertson, McGraw-Hill, New York, in press, 1971.

Sass, J. H., and R. J. Munroe, Heat flow from deep boreholes on two island arcs, *J. Geophys. Res., 75,* 4387–4395, 1970.

Sass, J. H., P. G. Killeen, and E. D. Mustonen, Heat flow and surface radioactivity in the Quirke Lake syncline near Elliot Lake, Ontario, Canada, *Can. J. Earth Sci., 5,* 1417–1428, 1968a.

Sass, J. H., A. H. Lachenbruch, G. W. Greene, T. H. Moses, Jr., and R. J. Munroe, Progress report on heat-flow measurements in the western United States (abstract), *Eos Trans. AGU, 49,* 325–326, 1968b.

Sass, J. H., R. J. Munroe, and A. H. Lachenbruch, Measurement of geothermal flux through poorly consolidated sediments, *Earth Planet. Sci. Lett., 4,* 293–298, 1968c.

Sass, J. H., A. H. Lachenbruch, and R. J. Munroe, Thermal conductivity of rocks from measurements on fragments and its application to heat-flow determinations, *J. Geophys. Res., 76,* 3391–3401, 1971.

Snavely, P. D., Jr., R. D. Brown, Jr., A. E. Roberts, and W. W. Rau, Geology and coal resources of the Centralia Chehalis district, Washington, *U.S. Geol. Surv. Bull., 1053,* 159 pp., 1958.

Spicer, H. C., Geothermal gradients and heat flow in the Salt Valley anticline, Utah, *Boll. Geof. Teor. Appl., 6,* 263–282, 1964.

Uyeda, Seiya, and Ki-iti Horai, Terrestrial heat flow in Japan, *J. Geophys. Res., 69,* 2121, 1964.

Von Herzen, R. P., and A. E. Maxwell, The measurement of thermal conductivity of deep-sea sediments by a needle probe method, *J. Geophys. Res., 64,* 1557–1563, 1959.

Von Herzen, R. P., and Seiya Uyeda, Heat flow through the eastern Pacific floor, *J. Geophys. Res., 68,* 4219–4250, 1963.

Walsh, J. B., and E. R. Decker, Effect of pressure and saturating fluid on the thermal conductivity of compact rock, *J. Geophys. Res., 71,* 3053–3061, 1966.

Waring, G. A., Thermal springs of the United States and other countries of the world, a summary, *U.S. Geol. Serv. Prof. Pap., 492,* 1965.

Warren, R. E., J. G. Sclater, Victor Vacquier, and R. F. Roy, A comparison of terrestrial heat flow and transient geomagnetic fluctuations in the southwestern United States, *Geophysics, 34,* 463–478, 1969.

Winograd, I. J., and William Thordarson, Structural control of groundwater movement in migeosynclinal rocks of south-central Nevada, in *Nevada Test Site, Mem. 110,* edited by E. B. Eckel, pp. 35–48, Geological Society of America, Boulder, Colo., 1968.